NOAA TM NWS TDL-46
13273

A UNITED STATES DEPARTMENT OF COMMERCE PUBLICATION

# NOAA Technical Memorandum NWS TDL-46

U.S. DEPARTMENT OF COMMERCE
National Oceanic and Atmospheric Administration
National Weather Service

COASTAL ZONE
INFORMATION CENTER

# SPLASH (Special Program To List Amplitudes of Surges From Hurricanes) I. Landfall Storms

CHESTER P. JELESNIANSKI

U.S. National Oceanic and Atmospheric Administration
National Weather Service

QC
851
.U6
T3
no.46

NOAA TECHNICAL MEMORANDA

National Weather Service, Techniques Development Laboratory Series

The primary purpose of the Techniques Development Laboratory of the Office of Systems Development is to translate increases of basic knowledge in meteorology and allied disciplines into improved operating techniques and procedures. To achieve this goal, the Laboratory conducts and sponsors applied research and development aimed at the improvement of diagnostic and prognostic methods for producing weather information. The Laboratory performs studies both for the general improvement of prediction methodology used in the National Meteorological Service System and for the more effective utilization of weather forecasts by the ultimate user.

NOAA Technical Memoranda in the National Weather Service Techniques Development Laboratory series facilitate rapid distribution of material which may be preliminary in nature and which may be published formally elsewhere at a later date. Publications 1 to 5 are in the former series, Weather Bureau Technical Notes (TD), Techniques Development Laboratory (TDL) Reports; publications 6 to 36 are in the former series, ESSA Technical Memoranda, Weather Bureau Technical Memoranda (WBTM). Beginning with TDL 37, publications are now part of the series NOAA Technical Memoranda, National Weather Service (NWS).

Publications listed below are available from the National Technical Information Service, U.S. Department of Commerce, Sills Bldg., 5285 Port Royal Road, Springfield, Va. 22151. Price: $3.00 paper copy; $0.95 microfiche. Order by accession number shown in parentheses at end of each entry.

ESSA Technical Memoranda

WBTM TDL 12 Charts Giving Station Precipitation in the Plateau States from 700-Mb. Lows During Winter. D. L. Jorgensen, A. F. Korte, and J. A. Bunce, Jr., October 1967. (PB-176 742)

WBTM TDL 13 Interim Report on Sea and Swell Forecasting. N. A. Pore and W. S. Richardson, December 1967. (PB-177 038)

WBTM TDL 14 Meteorological Analysis of 1964-65 ICAO Turbulence Data. DeVer Colson, September 1968. (PB-180 268)

WBTM TDL 15 Prediction of Temperature and Dew Point by Three-Dimensional Trajectories. Ronald M. Reap, September 1968. (PB-180 727)

WBTM TDL 16 Objective Visibility Forecasting Techniques Based on Surface and Tower Observations. Donald M. Gales, October 1968. (PB-180 479)

WBTM TDL 17 Second Interim Report on Sea and Swell Forecasting. N. A. Pore and Lt. W. S. Richardson, USESSA, January 1969. (PB-182 273)

WBTM TDL 18 Conditional Probabilities of Precipitation Amounts in the Conterminous United States. Donald L. Jorgensen, William H. Klein, and Charles F. Roberts, March 1969. (PB-183 144)

WBTM TDL 19 An Operationally Oriented Small-Scale 500-Millibar Height Analysis. Harry R. Glahn and George W. Hollenbaugh, March 1969. (PB-184 111)

WBTM TDL 20 A Comparison of Two Methods of Reducing Truncation Error. Robert J. Bermowitz, May 1969. (PB-184 741)

WBTM TDL 21 Automatic Decoding of Hourly Weather Reports. George W. Hollenbaugh, Harry R. Glahn, and Dale A. Lowry, July 1969. (PB-185 806)

WBTM TDL 22 An Operationally Oriented Objective Analysis Program. Harry R. Glahn, George W. Hollenbaugh, and Dale A. Lowry, July 1969. (PB-186 129)

WBTM TDL 23 An Operational Subsynoptic Advection Model. Harry R. Glahn, Dale A. Lowry, and George W. Hollenbaugh, July 1969. (PB-186 389)

WBTM TDL 24 A Lake Erie Storm Surge Forecasting Technique. William S. Richardson and N. Arthur Pore, August 1969. (PB-185 778)

WBTM TDL 25 Charts Giving Station Precipitation in the Plateau States From 850- and 500-Millibar Lows During Winter. August F. Korte, Donald L. Jorgensen, and William H. Klein, September 1969. (PB-187 476)

WBTM TDL 26 Computer Forecasts of Maximum and Minimum Surface Temperatures. William H. Klein, Frank Lewis, and George P. Casely, October 1969. (PB-189 105)

(Continued inside back cover)

13272

U.S. DEPARTMENT OF COMMERCE
National Oceanic and Atmospheric Administration
National Weather Service

COASTAL ZONE
INFORMATION CENTER

NOAA Technical Memorandum NWS TDL-46

# SPLASH (SPECIAL PROGRAM TO LIST AMPLITUDES OF SURGES FROM HURRICANES) I. LANDFALL STORMS

Chester P. Jelesnianski

U.S. DEPARTMENT OF COMMERCE NOAA
COASTAL SERVICES CENTER
2234 SOUTH HOBSON AVENUE
CHARLESTON, SC 29405-2413

Property of CSC Library

U.S. National Oceanic + Atmospheric Services
National Weather Service.
QC851.U6 T3 no. 46
1676 1246
APR 0 8 1997

Systems Development Office
Techniques Development Laboratory

SILVER SPRING, MD.
April 1972

UDC 551 465 755 551.515.2(047)(75/76)

| | |
|---|---|
| 551.46 | Oceanography |
| .465 | Dynamics of sea |
| .755 | Storm surges |
| 551.5 | Meteorology |
| 515 2 | Tropical hurricanes |
| (047) | Case histories and reports |
| (75/76) | (Southeast States and Gulf States) |

CONTENTS

Abstract ..... 1

1. Introduction ..... 1

2. Symbols used ..... 3

3. Developing a method to approximate the peak surge ..... 4
   A. Preliminary number for peak surge ..... 5
   B. Correcting for in situ (two-dimensional) sea depths ..... 7
   C. Correcting for in-situ vector storm motion ..... 10

4. Examples of peak surge approximation ..... 12

5. Comments on approximating the peak surge ..... 17
   A. Locating the peak surge on the coast ..... 17
   B. Correcting for variation of latitude..... 18
   C. Correction factors ..... 18

6. Using the computer to display coastal storm surges ..... 19
   A. Displaying storm surge envelopes by computer output ..... 19

7. Further comments and conclusions ..... 23

Acknowledgments ..... 24

References ..... 24

Appendix 1: empirical and nomogram surge models ..... 25
   A. Correlations between precomputed and observed surges ..... 26
   B. Composite nomogram and statistical model ..... 29

Appendix 2: SPLASH ..... 31
   A. Mechanics of running the program ..... 31
   B. Meteorological data deck for the program ..... 32

Appendix 3: some do's, don'ts, and applications when forecasting storm surges..... 35
   A. Meteorological parameters ..... 36
   B. Geographical features of basins and their coastlines ..... 40
   C. Inundation ..... 45
   D. Continental Shelf width, depths, and grid spacing ..... 48
   E. Astronomical tide ..... 50

# SPLASH
# (SPECIAL PROGRAM TO LIST AMPLITUDES OF SURGES FROM HURRICANES)
# I. LANDFALL STORMS

Chester P. Jelesnianski
Techniques Development Laboratory,
Systems Development Office, NOAA, Silver Spring, Md.

ABSTRACT. Whenever a tropical storm threatens to strike a coast, it is desirable to have at hand an estimate of the height of the potential storm surge. Two separate methods (based on dynamics) to estimate or forecast the surge are developed. The first method in which precomputed nomograms are used is designed only to arrive at a peak surge value. Arguments for the nomograms are simple meteorological parameters.

In the second method, a dynamic model is used to compute surges along an entire coastline. Computations are done by an electronic computer; surface meteorological parameters are used as input to the operational program.

Qualitative explanations for the surge phenomena are interspersed throughout part I. The relative importance of various meteorological parameters, continental shelf topography, and coastal geography are discussed.

## 1. INTRODUCTION

Coastal high waters generated by tropical storms often are the cause of a significant fraction of total storm damage. Because the potential for destruction can be enormous, we should be familiar with the physics of these tides as well as with the available forecasting procedures. When abnormal situations not covered by forecasting techniques occur, an understanding of the nature of the storm tide will serve to guide the forecaster.

The total storm tide is the sum of astronomical and meteorologically induced tides or storm surges, the latter generated by storm-driving forces. For practical purposes, these two tides are assumed superimposed with no interaction between them. Thus, a mere addition of the astronomical tide to the storm surge might be sufficient for storm tide prediction.

This paper (part I) continues and expands upon Harris' (1959) forecasting guide. Two simple forecasting techniques are given herein. In the first, precomputed nomograms are employed to find quickly the expected peak surge only. In the second, an off-the-shelf computer program, SPLASH, is used to compute the expected surges along segments of the east and gulf coasts of the United

States. At present, only storms that are expected to cross coastlines will be considered. A future paper (part II) will deal with storms moving along a coast.

Can the storm surge be predicted with an acceptable degree of accuracy and confidence? The answer in most cases is yes--if we understand the limitations of available models. One of the most serious limitations is meteorological. Although simple input parameters are used, determining their values is not always easy. One such parameter is the landfall point of storms; this is easy to visualize but difficult to forecast. Another parameter is the storm's central pressure, also used in the storm's size and vector motion. The forecast of storm surges will stand or fall on how well these parameters are known before the storm strikes the coast. In addition, for planning, a climatology of parameters can be used to form probability predictions of storm surges (Myers 1970).

Prior to the computer age, solutions to tidal hydraulic problems such as storm surges were arrived at by empirical means or by the use of simplified mathematical models. Both procedures are limited, the empirical approach because of a paucity of data, the other because of simplified assumptions. Today, sophisticated dynamic models can be handled on the computer numerically.

A companion study to this paper, Jelesnianski (1967) describes the dynamic model used here. The model can and does use two-dimensional variable depth basins and two-dimensional driving forces in motion. There are some severe restrictions to the solutions since curvilinear boundaries, bays, estuaries, islands, capes, spits, jetties, etc., are not considered. These geographical formations give rise to unknown <u>local</u> perturbations on the open coast storm surge. Best results occur for straight line coasts (with land elevations sloping strongly upward).

The sea-surface response to meteorological forces gives rise to surges on and along the coast; the assemblage of these coastal surges, for any given time, is called a <u>storm surge profile</u>. We regard this profile as a snapshot of tide heights along the coast. It builds and abates with time; it also can go through some erractic variations if storm motion is specialized or if the forces vary strongly with time. In any profile, some points may be experiencing highest surge while others will not as yet have experienced it. The curve made up of the highest (or upper) surges at each point over the entire storm duration is called a <u>storm surge envelope</u>; in general, it is not a profile but nevertheless is important in assessing inland flood potential.

Usually, the significant profile or envelope length on the coast is not much larger than the diameter of the storm. This means that affected coast lengths are generally small and could be represented by a tangent line meeting the coast at or near the point of landfall. This is true only if the geographical curvature of the coast relative to storm size is small; most of the east and gulf coasts do have gentle curvature. Contrary examples would be the irregular coasts of Japan, the Philippines, or East Pakistan.

To satisfy one objective (to forecast quickly an approximate value for the peak surge), we prepared three precomputed nomograms. To satisfy the other

objective (to describe quantitatively the storm surge profile along the coast and its peak surge value and position on the coast), we need access to a computer.

For the present, the assessment of changes in the profile due to local irregularities in the geometry of the coast will depend on the experience and artistry of the surge forecaster. In most cases, the local changes are not overwhelmingly significant; the errors in meteorological parameters used will most likely have a greater effect on the forecast. A substitute for experience is a technical paper by Harris (1963) that gives accounts of many historical surges; this reference should be in the library of all those engaged in storm surge forecasting.

## 2. SYMBOLS USED

Only ordinary arithmetic is employed in this paper. Some symbolism, however, is required for terms in the figures and arithmetic statements; these appear in table 1.

Table 1.--Symbols and their meanings

| | |
|---|---|
| $S$ | Surge on coast |
| $SS$ | Peak surge on coast |
| $S_p$ | Preliminary number for peak surge |
| $P_o$ | Central pressure (in mb) of tropical storm |
| $P_{oo}$ | Peripheral or outside ambient pressure (in mb) of storm |
| $\Delta P$ | Pressure drop (in mb) of storm (i.e., $P_{oo} - P_o$) |
| $\delta P$ | Variation of pressure drop (i.e., difference of two separate choices for $\Delta P$) |
| $R$ | Distance (in st.mi.) from storm's center to circle of maximum winds |
| $R_C$ | Radius of curvature of coast |
| $U_S$ | Speed (in mi/hr) of storm's motion |
| $F_G$ | Correction factor for local bathymetry along gulf coast |
| $F_E$ | Correction factor for local bathymetry along east coast |
| $F_M$ | Correction factor for vector storm motion |
| $D_S$ | Distance to peak surge from landfall point |
| $D$ | Depth at any point on Continental Shelf |
| $D_o$ | Finite sea depth at coast, obtained when general shelf profile is extended to coast |
| $l$ | Short length ($\ll R$), running seaward and from coast, where slope of depth profile greatly exceeds general slope of Continental Shelf |
| $l_o$ | Short length ($\ll R$), running landward and from coast, up to terrain heights that equal peak surge |
| $\rho$ | Correlation coefficient |
| $\theta$ | Angular measure from coastline to track of storm, where track terminates at landfall point |

## 3. DEVELOPING A METHOD TO APPROXIMATE THE PEAK SURGE

Conner et al. (1957) designed a simple empirical model to forecast storm surges. They plot observed[1] maximum tides against lowest observed[2] central pressure ($P_o$) and then find the line of best fit. Their correlation coefficient for 30 data points is 0.68. The data are for the Gulf of Mexico only, where the astronomical tide is less than a foot above mean sea level (MSL) and rarely exceeds 2 ft. Essentially, their model assumes that all storms are the same except for central pressure, that all storms strike coasts in the same relative way, and that the depth contours off all coasts are the same.

Harris (1959) expanded on this model to storms making landfall on the east and gulf coasts. He removed the seasonal sea-level anomaly, whenever possible, from the observed high waters. He also considered as parameters the peripheral storm pressure ($P_{oo}$), the size of the storm (R), the vector storm motion ($U_s$,$\theta$), and the distance of the 50-fm line from shore. For the available data, he found systematic variations of the surge with two parameters: the central pressure and the distance of the 50-fm line from shore. His correlation coefficient for 52 data points was 0.75.

Describing an objective forecasting scheme for the peak surge only, which reflects the above empirical models, will be done through precomputations in which our dynamic model is used. Here, the storm size R plays a minor role, just as in Harris' model; but the bathymetry[3] and vector storm motion play significant roles. Qualitative explanation will be given for some of the physics involved in surge generation.

For future reference, we make two definitions:

Standard basin. A basin with a straight coastline in which the depth profile seaward is a linear slope. The slope is the same along the entire coast (i.e., one-dimensional). Such a slope is shown in the inset of figure 2A. The basin can be considered a hypothetical mean for all basins.

Standard storm motion. A storm motion with a speed of 15 mi/hr and a track normal to the coast from sea to land. The storm must move onto land. This motion can be considered a hypothetical mean motion for all storms.

---

[1]Hoover (1957) subjectively alters some of the surge data. His experience suggests surge values higher than those reported. He arrives at an upper maximum surge profile between observed values. This subjective analysis gives him a correlation coefficient of 0.81. He does not alter surges for all storms, nor does he consider as many storms as Conner et al. (1957).

[2]Lowest central pressures were rarely observed. Instead, estimates were used (Weather Bureau 1957); and published data are scattered in the Monthly Weather Review.

[3]In our use of bathymetry, we mean bottom topography. These depths are given by marine coastal charts.

## A. Preliminary Number for Peak Surge

Harris (1959) in his empirical model finds little variation of the surge with the outside ambient air pressure $P_{oo}$ and sets it as a constant. In our dynamic model, $P_{oo}$ need not be constant. It is not difficult to obtain $P_{oo}$. One way to do this is with a surface weather chart. Move outward from the storm center to the first anticyclonically turning isobar and mentally record the pressure; do this for several directions from the storm center. The mean of your several pressure readings is $P_{oo}$. If the isobar patterns do not lend themselves to this technique, then use any mean pressure for the area or even a constant 1012 mb.

To develop a scheme initially patterned on empirical models, we go to the dynamic model (via computer) and ask it a preliminary question--what maximum surges do I obtain with the following constraints?

1. There are sets of storms; in each set, the radius of maximum wind R is constant.

2. In each set of storms, only the pressure drop ($\Delta P = P_{oo} - P_o$) is varied.

3. All storms have a standard motion.

4. All storms traverse a standard basin.

5. All storms make landfall at 30°N.

The computer's answer to this question is shown in figure 1; it is our first nomogram for quickly determining the expected peak surge.

Entering the nomogram with arguments $\Delta P$ and R gives a <u>preliminary</u> number. Later, this number will be revised with relaxation of constraints 3 through 5. In its present form, however, the preliminary number can be used as a crude estimate of the peak surge. When correlated with observed surges (appendix 1), it gives a correlation of 0.54 (i.e., the nomogram of fig. 1, which does not use all the information available about the storms, is not as efficient a predictor as the empirical models of Conner et al. 1957 and Harris 1959). Understanding this nomogram, however, will give us a better physical insight into surges.

For constant R, each curve is nearly a straight line passing through the origin; this means the predicted surge has relative error = $\delta P/\Delta P$, where $\delta P$ is a variation or error in the pressure drop. For example, a 1-mb error in pressure drops of 100 and 50 mb gives a storm surge error of 1 and 2 percent, respectively. This immediately indicates how accurate the pressure readings should be.

If $\Delta P$ is constant, the surge is weakly or mildly dependent on R accordingly as $\Delta P$ is small or large (i.e., the peak surge is quasi-conservative with re-

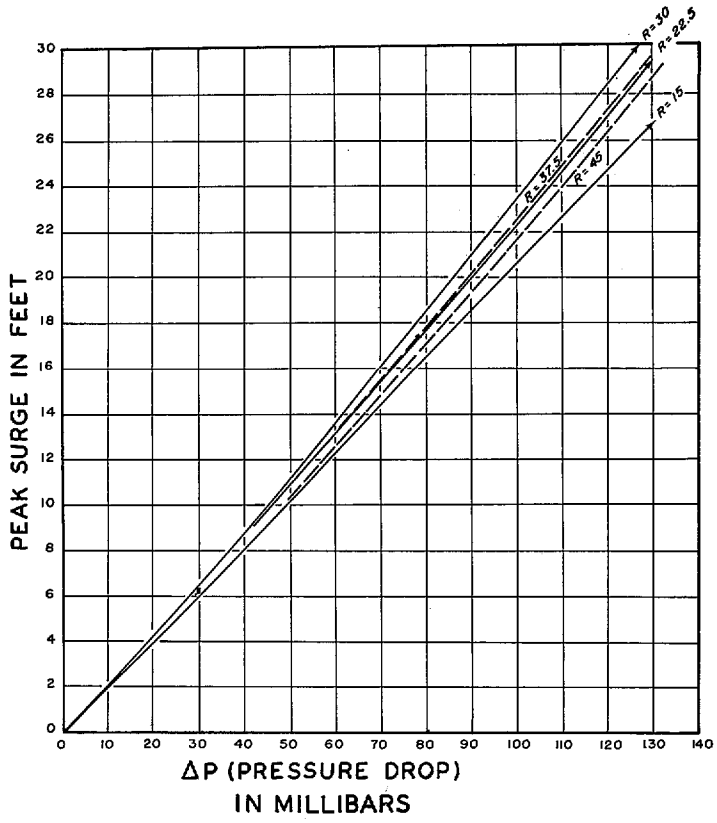


Figure 1.--Nomogram of peak surge on the open coast as a function of pressure drop and radius of maximum winds (R in st.mi.). The curves are computed for a standard storm motion across a standard basin.

spect to R). This is a most useful property because R is difficult to ascertain, especially for storms with double eye structures. For constant $\Delta P$ in figure 1, the peak surge reaches its maximum value for R at or slightly greater than 30 mi. We do not explain this behavior, except to state that, in our model, there is a critical storm size for a given storm speed that generates an upper maximum surge; similarly for a given storm size, there is a critical storm speed that generates an upper maximum surge.

Figure 1 is for a hypothetical standard basin shelf width of 72 mi. If we arbitrarily choose 50 fm (300 ft) to represent the shelf edge, the resulting shelf width along the east and gulf coasts ranges from 2 to 100 mi. Now noting that R rarely exceeds 50 mi for tropical storms, we have some clues for the applicability of figure 1:

1. If the shelf width is much smaller than the storm diameter of 2R (as occurs between the Florida Keys and Palm Beach) or if the shelf is much steeper than standard, then figure 1 is strongly distorted with respect to larger size storms.

2. If the shelf is much shallower than standard (as occurs at Eugene Isle, La., or Cedar Keys, Fla.), then figure 1 may be distorted with respect to medium to large size storms.

3. If an exceptionally large storm size occurs (i.e., R>50 mi), then figure 1 is out of range. This means that extratropical storms (in which R is normally very large) are excluded.

Large R's present many technical difficulties not considered here; we will only consider storms with R<50 mi. Here, we also take a pragmatic approach and assume that maximum surge is nearly independent of R along most coasts of the United States. One reason for restricting ourselves to the coasts of the United States is that shelf widths are generally greater than the radius of maximum winds for most tropical storms. In our model, the maximum wind[4] is a function of $\Delta P$ and R; hence, direct reference to it is not required.

We will now continue to explore some ways in which the remaining information about the storms can be used to improve forecasts. For the first of two corrections on the preliminary number, we remove the constraint of standard basin bathymetry; this is discussed in the next topic.

B. Correcting for In Situ (Two-Dimensional) Sea Depths

When a storm crosses a continental shelf, surges are not generated at once. Initially, driving forces will impart momentum to the sea; and any surface elevations are due mainly to static heights from pressure drop. To form waves such as a storm surge requires factors to transform the variable momentum in the sea (i.e., vorticity) into divergence. One such factor is the Coriolis force. However, it is not very effective for medium scale phenomena occurring under hurricanes. A much more effective factor is the bathymetry or sloping[5] depths of the continental shelf.

Harris (1959) empirically found systematic variations in the surge with variations in the distance of the 50-fm line from shore. Using this crude parameter, however, he could not refine the variations caused by dramatic changes in the bathymetry about the coast. Because the bathymetry along the coastline of the United States varies considerably, we might expect pronounced differences in storm surges at local coastal points, when all other things are equal. To see how bathymetry in our model affects coastal surges and also how to correct for it, we direct a second question to the dynamic model via computer--if one is given two storms (one for the gulf coast and the other for the east coast) with these constraints,

1. each storm has its own invariant $\Delta P$ and R[6] and

2. both storms have the same <u>standard</u> motion,

what is the ratio of peak surge at any point along the coastline of the United

---

[4]The average wind on a circle around the storm at radius R, <u>not</u> the <u>fastest mile</u> wind

[5]A limiting case is a vertical wall in a constant depth basin.

[6]For the gulf coast 55 mb and 15 mi. and for the east coast 68 mb and 30 mi. These values were chosen strictly for convenience, but they roughly reflect the differences in climatology between hurricanes in these areas.

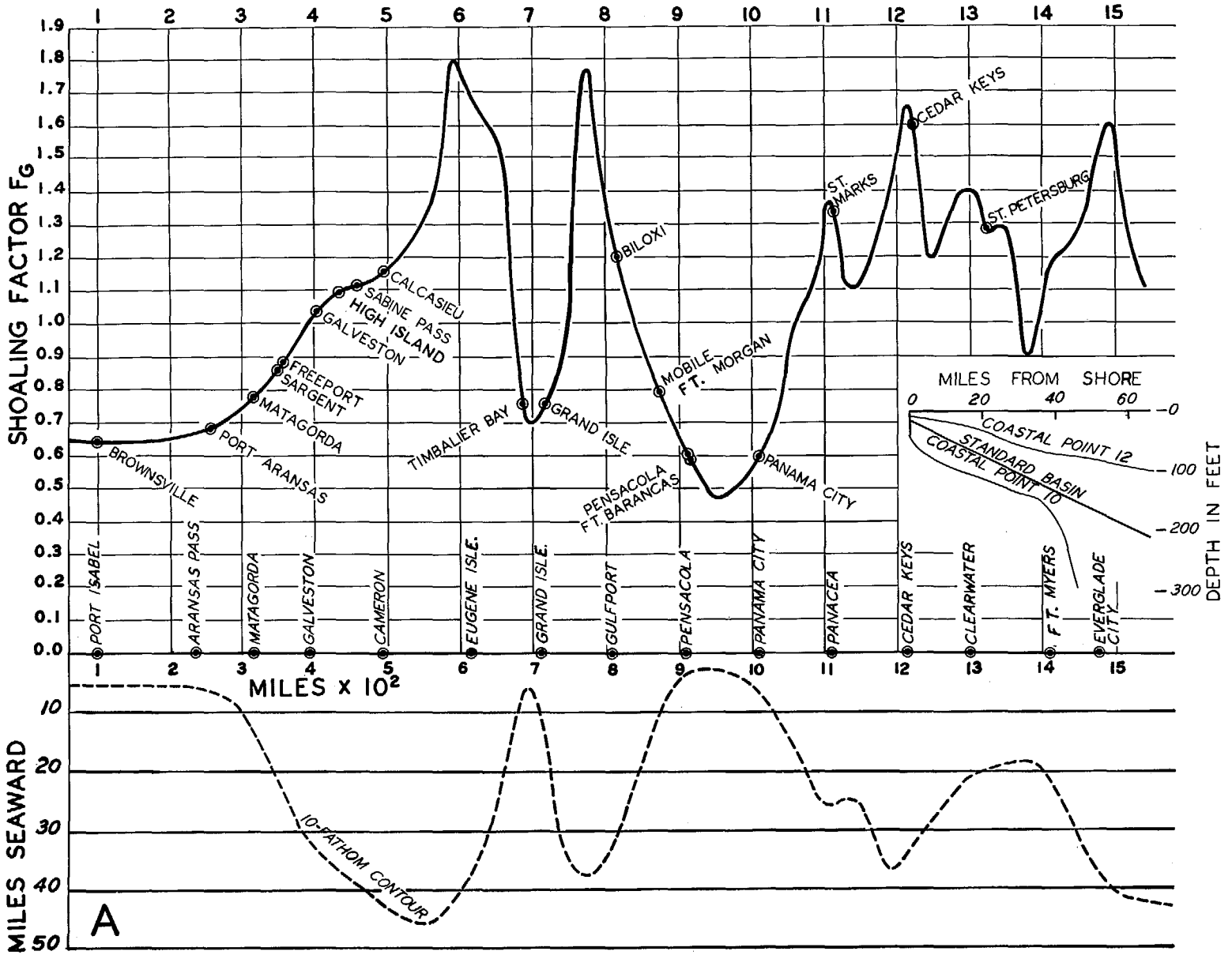


Figure 2.--Nomogram for shoaling factors along (A) the gulf coast and (B) the east coast

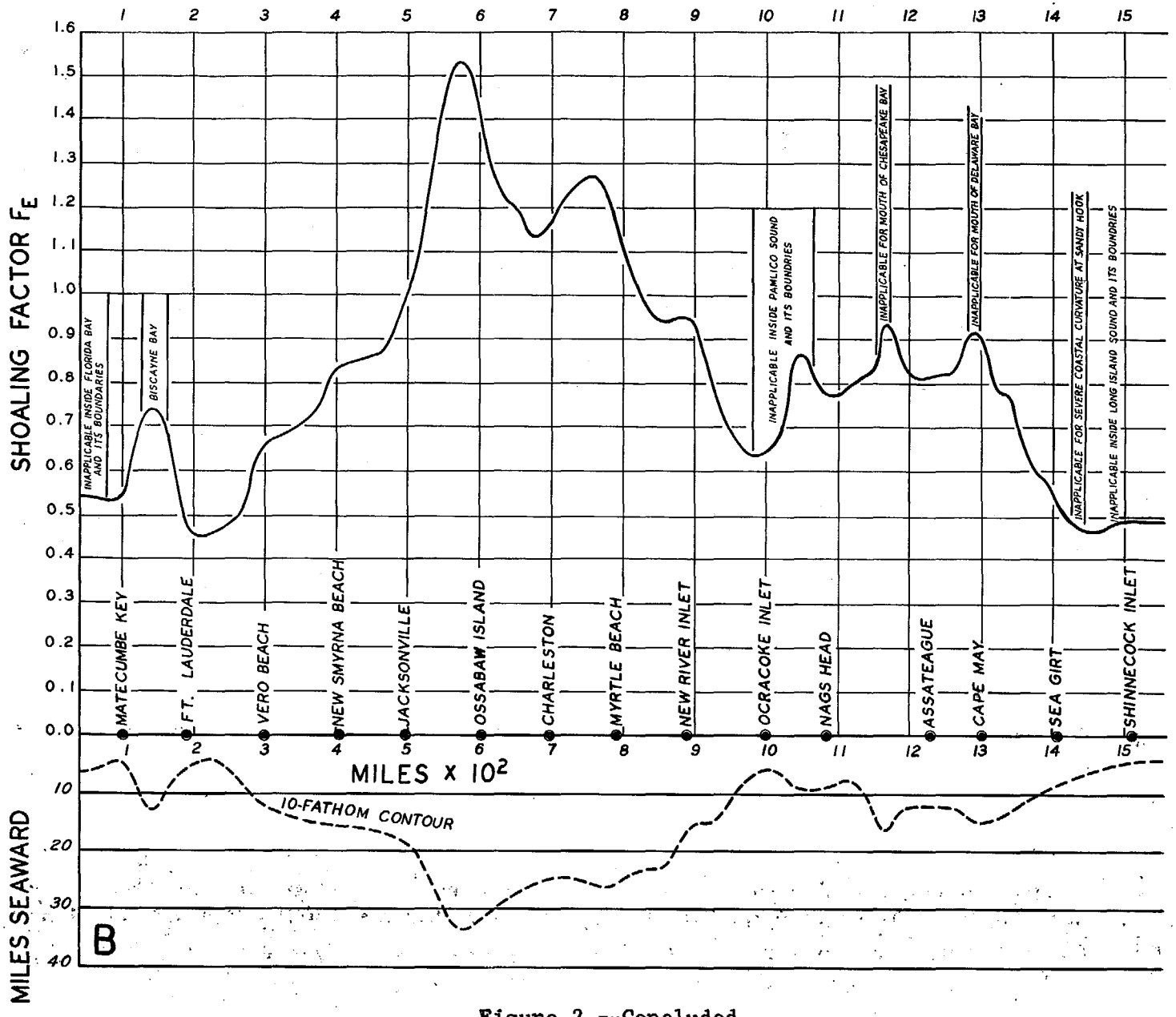


Figure 2.--Concluded

States to that of the peak surge in a standard basin located at 30°N?[7] The computer's answer to this question is broken into two parts,

1. the ratio $F_G$ for the gulf coast (fig. 2A on p. 8), and

2. the ratio $F_E$ for the eastern seaboard (fig. 2B).

In figure 2A, the vertical lines are 100 mi apart. Selected coastal cities are shown along the abscissa. The inset compares the steepest and the shallowe depth profiles in the gulf against the standard depth profile. The shoaling curve varies inversely as the distance of the 10-fm curve from the coast. In figure 2B, the shoaling curve between the Florida Keys and Vero Beach is speculative because the Continental Shelf differs greatly from standard. The factors are for the open coast surge and not for interior points.

Figure 2, our second nomogram, is used with figure 1 to determine the expected peak surge. For different constraints, the ratios or shoaling factor[8] $F_G$, $F_E$ will vary; but the variation in most cases, but not all, will be small. We pragmatically accept the shoaling factors as a working tool to correct for the local bathymetry. The preliminary number obtained from the nomogram of figure 1 is multiplied by the shoaling factor obtained from figure 2. Note in figure 2 that the distance of the 10-fm depth curve from the coast is a rough inverse measure of the shoaling factor.

If we correlate the preliminary number, revised for shoaling, against the data points of appendix 1, the correlation coefficient is 0.68, a significant improvement in correlation. Note especially that some of the preliminary numbers have been radically altered by the shoaling curve. The stage is now set for another revision.

For the second of two corrections on the preliminary number, we remove the constraint of standard storm motion; this is discussed in the next topic.

### C. Correcting for In-Situ Vector Storm Motion

Harris (1959) found systematic variations of the surge for two parameters, $P_o$ and a crude estimate of the bathymetry. His distribution of data points was inadequate to permit him to derive systematic variations for vector storm motion.

---

[7] We have incorporated corrections for latitude or Coriolis effects in the ratios or shoaling factors.

[8] To develop the shoaling curve (fig. 2), we used the following procedure. The same storm was made to reach land at equidistant points along the coast, at the rate of three storms per 100 mi. The envelopes of the computed surges were then drawn along the coast. Finally, the envelope of the envelopes was drawn by hand. This hand-drawn envelope was then rescaled, for a non-dimensio ratio, using the computed peak surge in a standard basin. The shape of this envelope, or shoaling curve, depends mildly on the storm size R.

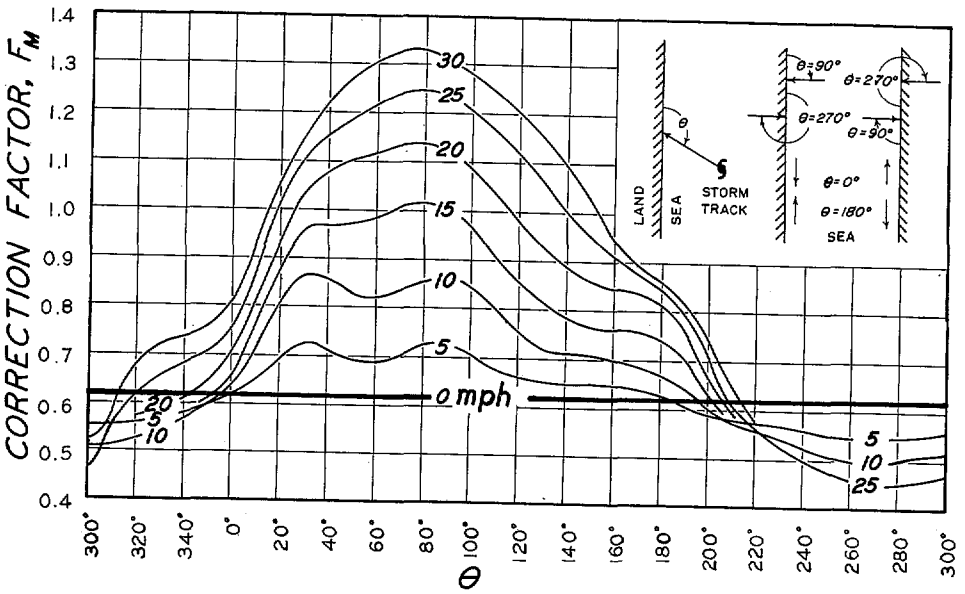


Figure 3.--Nomogram of correction factors against the vector storm motion. The factor corrects for motion other than standard; standard motion is a vector track, 090°/15 mph, relative to the coastline. The inset gives orientation of the argument θ and also gives some extreme tracks relative to the coast.

In our model, the track of a storm influences surge generation. There exists a critical motion relative to a coast that gives the highest possible surge under any given set of conditions. The critical speed generally is greater than 30 mi/hr; it will be less only with exceptionally small storms or in exceptionally shallow and wide basins. Storms reaching land rarely attain a critical speed; thus, we will not consider it here.

To correct for the effect of different vector motions on coastal surges, we direct a third question to the dynamic model via computer--if one is given storms traveling at any direction and speed relative to a coast and these constraints,

1. all storms have R = 22.5 mi and ΔP = 62 mb and

2. all storms traverse a <u>standard</u> basin,

what is the ratio of the generated peak surge to that generated by a storm with standard motion? The computer's answer to this question, in terms of the ratio or motion factor $F_M$, is given in figure 3; the insets define a direction θ that is the angle of the storm's track relative to the coast. We mentally orientate ourselves along the coast with the right side seaward, left side landward, and facing 0° direction; θ is then measured clockwise from shore to track, where the track terminates at the landfall point.[9] The figure is only

[9] We arbitrarily assign a latitude of 30°N at this point and let the Coriolis parameter be constant; latitude changes are accounted for in the shoaling curve (fig. 2).

DATA

____ STORM: name of storm

____ DATE : day, month, year

____ HOUR : local time of landfall

____ STAT : nearest station to landfall point
see figure 5 for position of stations

____ MILES: distance to landfall from STAT

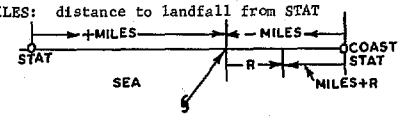


____ R : radius of max winds in miles,
$10 < R < 50$

____ MPR : MILES + R, distance to peak surge from STAT

____ $P_{oo}$ : mean ambient air pressure about storm

____ $P_o$ : central pressure of storm

____ $\Delta P$ : $P_{oo}-P_o$, the pressure drop of storm

____ $U_S$ : speed of storm on shelf

____ $\theta$ : angle from coast to storm track

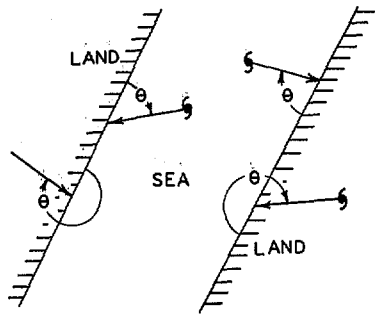


$\theta$ is measured from coast, seaward to track

PRECOMPUTED VALUES

____ $S_p$ : the preliminary number
enter figure 1 with arguments $\Delta P$ and R

____ $F_G, F_E$ : correction factor for shoaling
enter figure 2 with argument STAT + MPR
for location of peak surge on coast

____ $F_M$ : correction factor for vector storm motion
enter figure 3 with arguments $U_S$ and $\theta$

COMPUTATIONS

____ SS : the expected peak surge in feet

SS = ( )·( )·( )

$S_p$ $F_G$ $F_M$ gulf coast

$S_p$ $F_E$ $F_M$ east coast

____ $1/\Delta P$ : relative surge error per mb error
example: $\Delta P$ = 50 mb
$1/\Delta P = 0.02 = 2\%$
5-mb error means 10% surge error

NOTE: SS should be superimposed with astronomical tide at time of landfall. Use C&GS Tide Tables; use MSL datum.

Figure 4.--A form to obtain expected peak surge from precomputed nomograms

speculative for storms crossing the coast with a small acute angle (i.e., for $\theta = 0°$ or $\theta = 180°$). For different constraints, the motion factor $F_M$ will vary, but in most cases only slightly[10]; we pragmatically accept the motion correction as a working tool. This figure is our third and last nomogram to quickly determine the expected peak surge. The product of $S_p$ and $F_G$ (or $F_E$) obtained by use of the first two nomograms is multiplied by $F_M$.

If we correlate the preliminary number, revised for shoaling and storm motion, against the observed data points (appendix 1), the correlation coefficient is 0.85.

## 4. EXAMPLES OF PEAK SURGE APPROXIMATION

To quickly construct the expected peak surge value, one must introduce three nomograms; two of these require special orientation procedures. As an aid for use with the nomograms, we suggest a computational form such as shown in figure 4. The form is broken into three parts. The first part, DATA, composes entry

[10] If basins have much steeper sloping depths than the standard basin or the vector storm motion is significantly different than standard, then $F_M$ as given by figure 3 is exaggerated; the opposite is true if the basin slope is much shallower than standard.

arguments for the nomograms. The second part, PRECOMPUTED VALUES, lists numbers from the nomograms. The third part, COMPUTATIONS, uses these numbers to compute the peak surge value.

In the data part of the form, $\Delta P$ and R are self explanatory: these are entry arguments for the first nomogram (fig. 1) to derive the preliminary number $S_p$. This is then entered in the precomputed values part of the form.

In the data part of the form, the geographical location of the expected peak surge requires some explanation. We need this location for an entry argument in the second nomogram (fig. 2) to extract the shoaling factor number $F_G$ or $F_E$. To find this location, we suggest:

1. Consider preselected geographical stations on the gulf and east coasts (table 2 or fig. 5); these stations are approximately 100 st.mi. apart.

2. Select the nearest station to the given landfall point; call it STAT.

3. Let the observer at sea face land with coastlines to his right and left.

4. Measure the distance in MILES from the station to the landfall point on the coast.

   a. Use negative MILES if landfall is left of STAT.
   b. Use positive MILES if landfall is right of STAT.

5. Find MPR by adding MILES and R; this gives the approximate location of the peak surge relative to STAT.

We enter the second nomogram at STAT; then move away from it the distance MPR on the abscissa; if MPR is negative, then move to the left. Now move vertically to the shoaling curve, then horizontally to the ordinate; read off the shoaling factor number $F_G$ or $F_E$. This is then entered in the precomputed values part of the form.

In the data part of the form, the angle $\theta$ from coast to storm track requires some explanation. We need this angle as an entry argument for the third nomogram (fig. 3); this is necessary to extract the correction factor $F_M$ for arbitrary storm motion. We are not so much interested in the compass direction of storm motion as we are in relative direction to the coast. The simplest way to derive this direction is to measure it directly by protractor on a historical or weather prognostic chart where the track is given; we remark that a tanget line to the coast must be drawn at, say, landfall point. Here, the observer is orientated so that sea is to his right and land to his left; he then measures $\theta$ clockwise from the coast to where the track terminates at the landfall point. Note that the track can run from land to sea for exiting storms; in such cases, $\theta > 180°$.

We enter the third nomogram with $\theta$ and the storm speed $U_S$, and we read off the correction factor number $F_M$. This is then set in the precomputed values part of the form. The remainder of the form is self explanatory.

Table 2.--Preselected coastal stations*

| GULF STATIONS | LATITUDE | LOGITUDE | EAST CST STATS | LATITUDE | LONGITUDE |
|---|---|---|---|---|---|
| PT ISABEL | 26 05N | 97 10W | MATCMB KEY | 24 55N | 80 39W |
| ARANSAS PS | 27 50N | 97 03W | FT LAUDRDL | 26 07N | 80 06W |
| MATAGORDA | 28 21N | 96 24W | VERO BEACH | 27 39N | 80 21W |
| GALVESTON | 29 16N | 94 48W | N SMYRNA BCH | 29 02N | 80 54W |
| CAMERON | 29 46N | 93 19W | JACKSNVLLE | 30 20N | 81 24W |
| EUGENE ILE | 29 21N | 91 24W | OSSABAW IS | 31 46N | 81 04W |
| GRAND ISLE | 29 13N | 90 01W | CHARLESTON | 32 44N | 79 51W |
| GULFPORT | 30 15N | 89 00W | MYRTLE BCH | 33 41N | 78 53W |
| PENSACOLA | 30 20N | 87 11W | N RIVER IN | 34 32N | 77 20W |
| PANAMA CTY | 30 07N | 85 42W | OCRCKE INL | 35 04N | 76 01W |
| PANACEA | 29 59N | 84 19W | NAGS HEAD | 36 01N | 75 39W |
| CEDAR KEYS | 29 11N | 83 02W | ASSATEAGUE | 37 54N | 75 20W |
| CLEARWATER | 27 59N | 82 49W | CAPE MAY | 38 55N | 74 54W |
| FORT MYERS | 26 29N | 82 10W | SEA GIRT | 40 08N | 74 02W |
| EVRGLD CTY | 25 45N | 81 30W | SHNNCK INL | 40 51N | 72 28W |

*These location abbreviations are exactly as used for input to SPLASH.

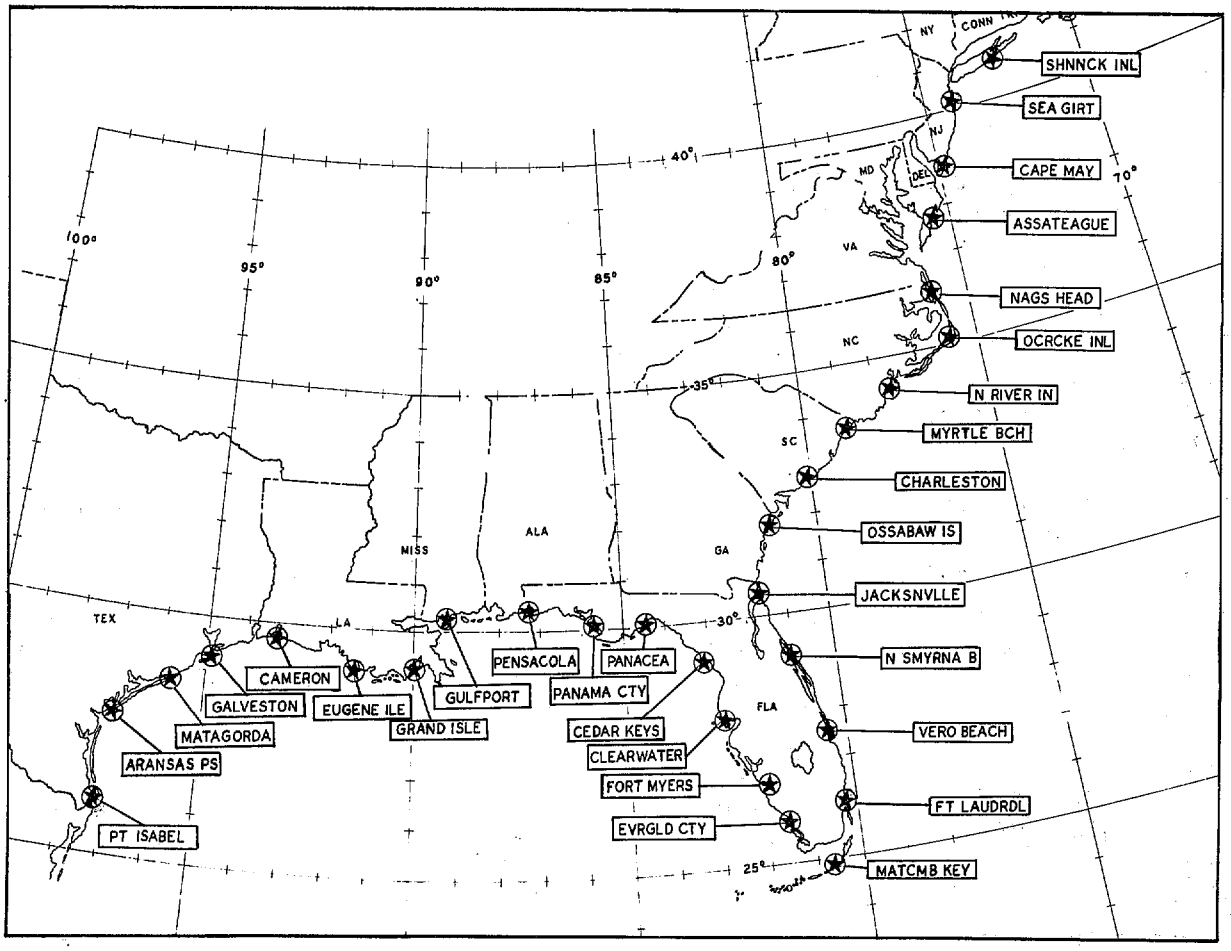


Figure 5.--Selected stations on the gulf and east coasts

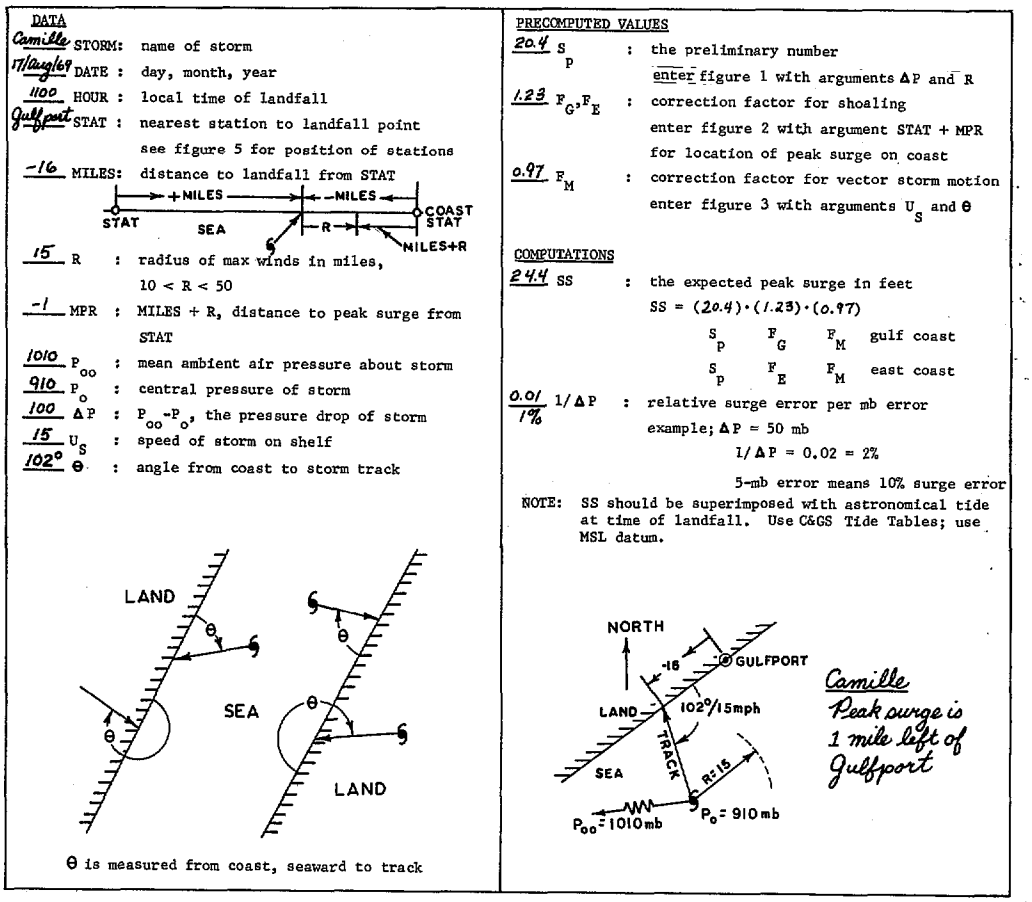


Figure 6.--Completed computation form for the expected peak surge value (hurricane Camille)

Hurricane Camille. One of the most devastating[11] storms of record in the Gulf of Mexico was hurricane Camille, 1969. For quickly computing the expected peak surge for this storm, we used the form shown in figure 6. In the DATA part of the form, the storm parameters were subjectively assembled from bulletins, advisories, historical weather maps, etc.;[12] official values for these parameters may be somewhat different. In the lower right-hand corner of the figure, we give a pictorial description of the meteorological parameters and geographical orientation of the storm reaching land. The computed peak surge value on the form is 24.4 ft; the astronomical tide at the time of landfall was negligible. This compares favorably with the highest observed tide of 24.6 ft near Pass Christian, La. We remark that different storm parameters may alter the computed peak surge significantly; for example, a 5-mb change in the central pressure means a 5-percent change in the expected peak surge.

[11] Hurricane Carla, 1961, might also share this dubious honor. Although not as intense as Camille, its much larger size generated significant surges along a remarkably long length of coast.

[12] The storm appeared to be filling as it approached the coast; hence, the mean central pressure on the shelf was used.

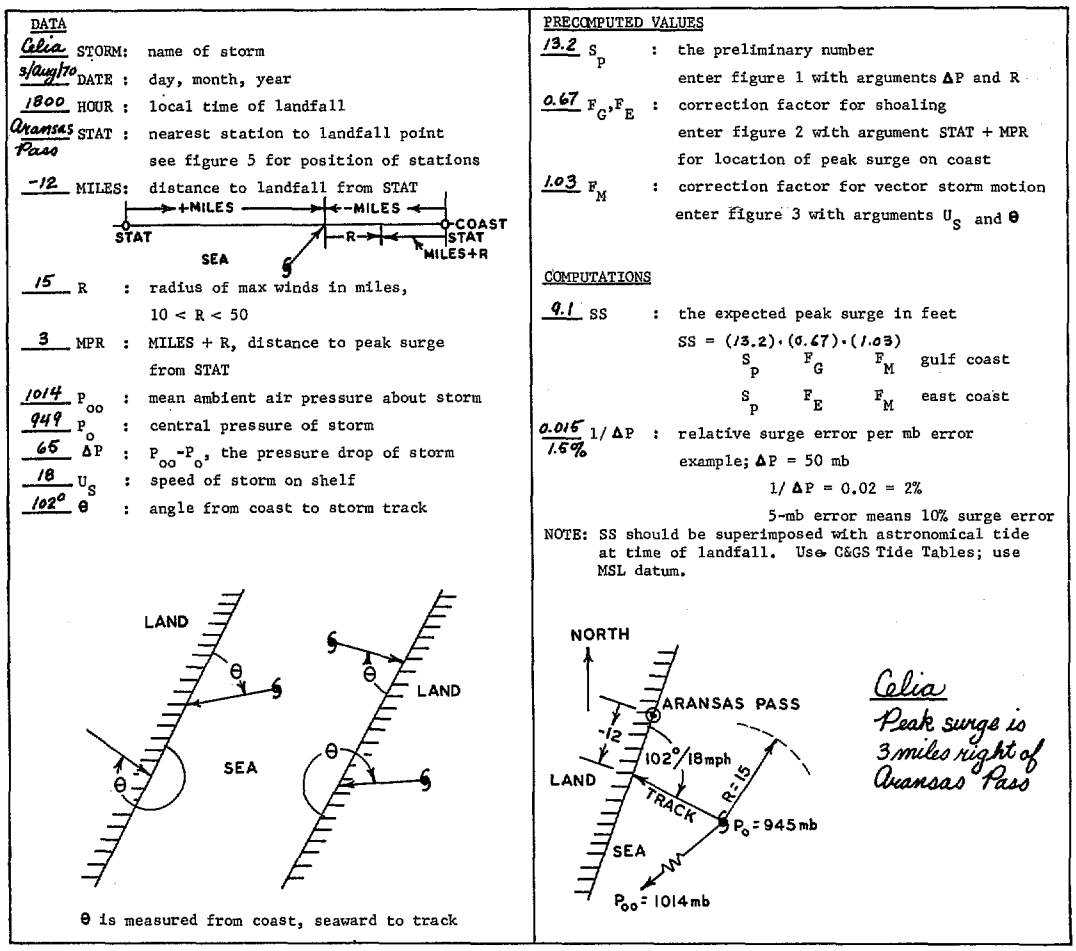


Figure 7.--Completed computation form for the expected peak surge value (hurricane Celia)

Hurricane Celia. A noteworthy feature of this storm was strong deepening of the central pressure prior to landfall. It is possible to program meteorological parameters as functions of time if such complexity is desired. Forecasting them, however, is problematical; and it is not easy to portray all combinations in simple and convenient form. What must be understood is that parameters varying strongly with time, in comparison with their mean values while the storm traverses the shelf, sometimes can generate larger surges. Most storms reaching land transverse the shelf quickly; thus, the parameters change insignificantly with time except, possibly, the central pressure. Accordingly for deepening storms, it is suggested that while the storm is on the shelf, the lowest central pressure be used.

For quickly determining the expected peak surge for Celia, 1970, we used the form shown in figure 7. In the data part of the form, the storm parameters were subjectively assembled as for Camille. The computed peak surge value on the form is 9.1 ft; the astronomical tide at the time of landfall was 0.3 ft, thus making the expected peak surge 9.4 ft. This compares favorably with the highest observed surge of 9.2 ft on the open coast. There were some higher surges 7 mi inland from the open coast, but our model does not consider local inland effects.

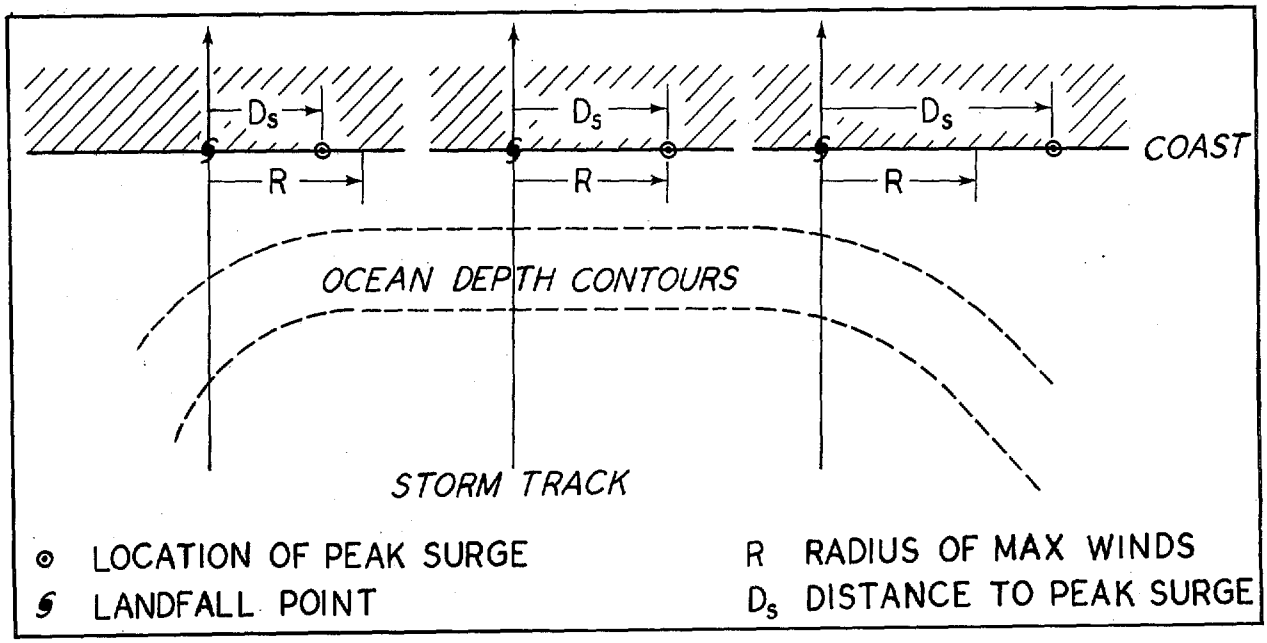


Figure 8.--Qualitative illustration showing the varying positions of peak surge on the coast as compared with two-dimensional bathymetry

## 5. COMMENTS ON APPROXIMATING THE PEAK SURGE

We should be aware of limitations when using precomputed nomograms to forecast the peak surge. Some of the limitations are as follows.

### A. Locating the Peak Surge on the Coast

If the storm track is about normal to the coast, then the peak surge will occur at a distance roughly equal to R, to the right of landfall (as viewed from the sea). We use this rule as a working criterion even though the peak surge position will vary for two reasons.

1. The distance to peak surge from landfall (call it $D_S$) is a function of the vector motion of the storm relative to the coast.

2. If the local bathymetry varies considerably about the landfall point, then $D_S$ also varies. Figure 8 describes this phenomena pictorially.

We make no attempt to apply these two phenomena (or other more subtle ones); the interrelations are too complicated for convenient expression. We point out that a landfall position on a steep portion of the shoaling curve of figure 2 will not only distort and stretch the surge profile but also relocate the peak surge on the open coast. Thus when using nomograms, the peak surge determination could be significantly in error. Generally, the absolute error $|D_S - R|$ is not large compared with R. More important, the predicted landfall error in most cases is much greater than $|D_S - R|$. If there is a desire to locate the peak surge and its value more precisely on the open coast for a particular storm, then the dynamic model should be run on the computer directly to find the storm surge profile.

## B. Correction for Variation of Latitude

The variation of storm surges due to variations in latitude is generally less than 10 percent for storms reaching land between 15° and 45°N. Because of this rather small variation either side of latitude 30°N, it was decided to incorporate latitude corrections directly with the shoaling curves of figure 2. The incorporated correction is not exact when the actual storm is greatly different from the storm used in the figure, but the sign of the correction is always proper.

We point out that for constant $\Delta P$ and R, the wind speed decreases (increases) with increasing (decreasing) latitude; similarly, for a constant wind profile, the $\Delta P$ increases (decreases) with increasing (decreasing) latitude. These effects are due to variations of the Coriolis parameter with latitude.

It is of some consequence whether we used a fixed maximum wind or a fixed pressure drop when computing the shoaling factors for a figure 2-type nomogram that incorporates changes in latitude. This is because the small changes caused by the Coriolis parameter can be opposite in sense. In most cases, pressures are more readily ascertained than wind; therefore, we suggest that $\Delta P$ be fixed and the winds permitted to vary with latitude. The user need not concern himself with winds; instead, he uses the pressure drop at or near the time of landfall--the wind effects are taken into account automatically.

## C. Correction Factors

The three nomograms (figs. 1-3) form an ad-hoc system for quick determination of useful numbers for the peak surge. These nomograms are not independent. While generally they are only weakly dependent, the dependency in isolated instances is sufficiently significant to yield sizable errors in the expected peak surge.

Why are the nomograms interdependent? The shoaling factors $F_G$, $F_E$ for nonstandard basins were computed using the convenient assumption that all storms of a given size move with standard vector motion; but for the storm motion factor $F_M$ for nonstandard motion, it was assumed that all storms have a given size and traverse a standard basin. What this means is that the meteorology and basin under consideration with a given storm must not be too far from standard and that the storm size R must be between 10 and 50 mi.

If the correction factors are considered to be first order, then the dependency between the nomograms is second order. We would like to give methods and values for higher order corrections, but the relations are no longer simple.

Such a complication is now discussed. In the nomogram of figure 1, in which all storms are assumed to travel with standard motion, we notice that, for a given $\Delta P$, the preliminary number $S_p$ reaches a maximum at a critical R of about 30 mi. This means that, for given travel speeds, we must concern ourselves with critical storm sizes; similarly, for a given storm size, we must concern ourselves with critical speeds. The critical situation, however, will vary as the geography of the continental shelves varies. This type of torturous feedback--one of many--makes it difficult to arrive at simple generalized methods for higher order corrections.

One possible method is to eliminate the nomogram for shoaling factors. This can be done by constructing particular nomograms for $S_p$ and $F_M$ at selected points of interest on the coasts; of course, the motion factor charts of $F_M$ should be constructed for storms of different sizes at each of the coastal points. In this way, the second-order corrections would be partially eliminated; but the effort and cost of doing this is staggering. Instead, we settle for warning the user of where to expect weaknesses when using these nomograms.

A quick and easy but not foolproof way to spot suspicious situations is by use of the shoaling curve. If you ascertain that the peak surge occurs near one of the troughs or crests of the shoaling curve, the shoaling factor deviates significantly from 1.0, and the vector storm motion is significantly different from standard, then the correction factors may be amiss.

We can avoid these uncertainties by direct machine computations that can be made for particular storms reaching land at particular coastal points. A method for doing this is described in section 6.

## 6. USING THE COMPUTER TO DISPLAY COASTAL STORM SURGES

The expected peak surge value, alone, gives no information as to how much of the coast will be affected by surges. We need coastal storm surge profiles, varying with time, to determine this. For operational conditions, direct computer computation using SPLASH is suggested. The mechanism for running this program is described in appendix 2; some limitations on the use of the resulting open coast surge profiles are described in appendix 3. Note that SPLASH is accessible for use in operational field forecasting.

Because local high water along an affected coast does not occur simultaneously with the peak surge, we must consider time variations in the profile. With the versatility of the computer, we can display the profile at successive times before and after the time of peak surge or display surge history at selected points on the coast, or both. For forecasting, we are more interested in high water heights along the affected coast than in time history; therefore, when using the computer, we settle for the envelope of coastal high water heights, disregarding the time of occurrence of local high water.

### A. Displaying Storm Surge Envelopes by Computer Output

An example of a programmed computer output is shown in figure 9. The graph displayed is the envelope of coastal high water heights for a storm reaching land.

The printed message beginning the output is a résumé of storm parameters selected by the programmer. For information, we also print out the maximum wind of the storm. This is a sustained, average wind for a stationary storm; as such, it should not be used for forecasting.[13]

The next message gives factors to update surges for a variation of the pressure drop, $\Delta P$. This factor corrects heights on the surge envelope if alternate

[13] This wind should not be confused with the "fastest mile" wind that is about 1.3 times greater.

pressure drops are used. The range of updated pressure is ±10 mb; it is incremented in 2-mb steps and added to the original pressure drop. We remark that it is unnecessary to rerun the program for small errors in pressure drop; the user merely multiplies the envelope surge heights with the correction factor for the updated pressure estimate.

The vertical scale of the graph is 20 ft. If the peak surge exceeds this, then the ordinate is rescaled to 40 ft.

The horizontal scale of the graph is 600 st.mi. long; it represents the coast on a straight line. The dots on the scale are 4 mi apart. On alternate dots, highest local surge heights are printed in feet. Just above, and near the middle of the scale, is a symbol ⌒*⌣; this represents the landfall position on the coast. Left and right of landfall, and below the dots, are linear distances in statute miles; below this are selected cities as they lie along the coast. The center of the horizontal scale is tangent to the natural coast; as such, it distorts and compresses distances on the curvilinear coast. This means that the printed distances away from the basin center are smaller than the actual curvilinear distances along the coast.

The graph itself is portrayed with asterisks. Only positive surges are printed. Negative surges do occur on the coast; if such information is desired, it could be displayed by a snapshot of the surge profile against time (i.e., a time history of the coastal surge). With storms reaching land, however, time surge profiles are less interesting operationally than the envelope of high waters. We cannot give a complete envelope because computations are terminated 3 to 9 hr (depending on storm speed) in real time after landfall occurs. This means that heights computed along the trailing ends of the envelope are slightly smaller than those that would be obtained with an infinite real-time run, especially for very slow storms traveling nearly parallel to the coast. Note that the ends of the envelope occur some distance from landfall where the effects of curvilinear coasts can become significant.

For operational planning, without resort to extensive recomputations, it is desirable to form an estimate of the surge if landfall occurs at a point other than the one originally forecast. To do this, we assume the original storm can strike anywhere on the coast, with the same constraints as for the original landfall.[14] We only need to compare the relative shoaling factors given in figure 2; the original envelope is then restructured with these relative shoaling factors.

The three horizontal scales that appear below the column of cities all display approximate surge heights. The first two give envelope surge heights for the storm reaching land 100 mi to the right and left of the original landfall. The last scale gives potential peak surge heights everywhere on the coast (i.e., a worst case estimate for each point on the coast). Note that when using the last scale, the peak surge is at about distance R to the right of the assumed landfall; exceptions[15] would be coastal areas where there are

[14] This means that the track orientation is always the same relative to coastal orientation at landfall point (i.e., $\theta$ of fig. 3 is constant).

[15] An example is given in appendix 3B, under the discussion of deltas and hurricane Betsy, 1965.

YOU HAVE SPECIFIED THE FOLLOWING STORM PARAMETERS

| | |
|---|---|
| LANDFALL POINT IS | 16 MILES LEFT OF GULFPORT |
| THE STORM IS MOVING TO THE | NNW AT 12.0 MPH |
| THE PRESSURE DROP IS | 100 MBS. |
| THE RADIUS OF MAXIMUM WIND IS | 15.0 STATUTE MILES |
| THE MAXIMUM (SUSTAINED) WIND IS | 136.7 MPH |

THE MAX WIND IS DERIVED FOR A (STATIONARY) STORM ON USING THE INPUT STORM PARAMETERS

IF YOU WANT TO UPDATE YOUR 100 MB PRESSURE DROP, USE THE FOLLOWING CORRECTION FACTORS ON THE COMPUTED SURGE VALUES

| UPDATED PRESSURE DROP | 90 | 92 | 94 | 96 | 98 | 100 | 102 | 104 | 106 | 108 | 110 |
|---|---|---|---|---|---|---|---|---|---|---|---|
| CORRECTION FACTOR | .89 | .92 | .93 | .96 | .97 | 1.00 | 1.01 | 1.04 | 1.05 | 1.08 | 1.10 |

STORM SURGE HEIGHTS (FEET)

35 30 25 20 15 10 5 0

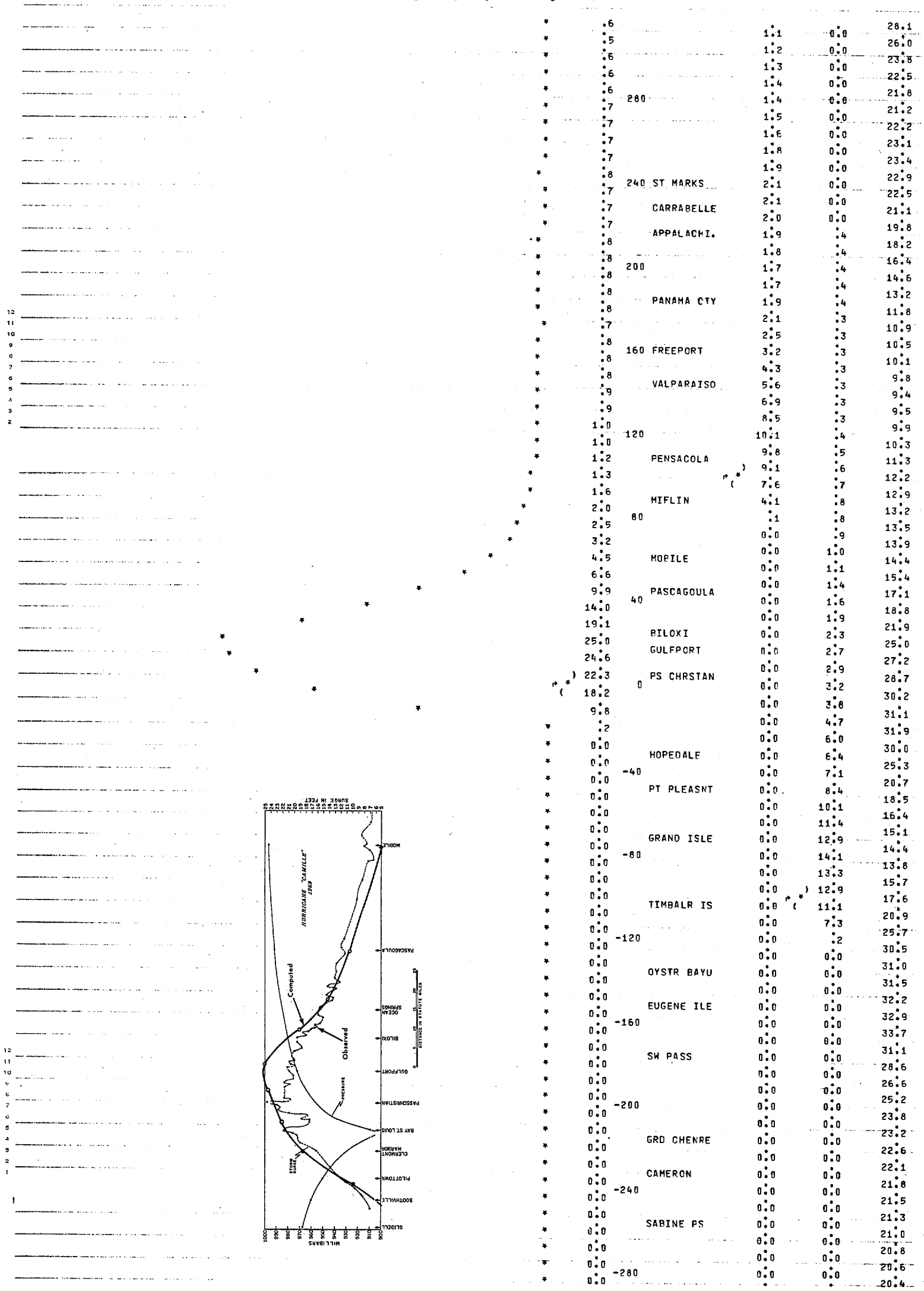


TIDE HEIGHTS ARE FT ABOVE MEAN SEA LEVEL.
HOURLY VALUES ARE PRINTED 12 HRS BEFORE TO 12 HRS AFTER ESTIMATED TIME OF LANDFALL.
ESTIMATED LANDFALL TIME 1000 LCL STD TIME, 17 AUG 1969 ESTIMATED TIME OF LANDFALL

| LCL STD TIME | 22 | 23 | 24 | 1 | 2 | 3 | 4 | 5 | 6 | 7 | 8 | 9 | 10 | 11 | 12 | 13 | 14 | 15 | 16 | 17 | 18 | 19 | 20 | 21 | 22 |
|---|---|---|---|---|---|---|---|---|---|---|---|---|---|---|---|---|---|---|---|---|---|---|---|---|---|
| PRT ST JOE | .2 | .3 | .3 | .4 | .4 | .3 | .3 | .2 | .2 | .1 | .1 | .1 | .1 | .2 | .2 | .3 | .3 | .3 | .3 | .3 | .3 | .3 | .3 | .4 | .4 |
| ST ANDR CH | .3 | .3 | .3 | .3 | .3 | .3 | .2 | .2 | .1 | .1 | .1 | .1 | .2 | .2 | .3 | .3 | .3 | .3 | .3 | .3 | .3 | .3 | .4 | .4 | .5 |
| PNSCL B EN | .2 | .2 | .3 | .3 | .3 | .3 | .2 | .2 | .1 | .1 | .1 | .1 | .1 | .2 | .2 | .2 | .2 | .2 | .2 | .2 | .2 | .2 | .3 | .3 | .4 |
| MOBILE PT | .1 | .2 | .2 | .2 | .2 | .2 | .1 | .1 | .0 | -.0 | -.0 | -.0 | .0 | .1 | .1 | .2 | .2 | .2 | .2 | .2 | .2 | .2 | .2 | .2 | .3 |
| PASCAGOULA | .3 | .3 | .4 | .4 | .4 | .4 | .3 | .2 | .2 | .1 | .1 | .1 | .2 | .2 | .3 | .3 | .3 | .3 | .3 | .3 | .3 | .3 | .3 | .4 | .5 |
| BILOXI | .3 | .4 | .4 | .5 | .5 | .5 | .4 | .3 | .2 | .2 | .1 | .1 | .2 | .2 | .3 | .3 | .4 | .4 | .4 | .4 | .4 | .4 | .4 | .5 | .5 |
| BRETON IS | .2 | .3 | .3 | .3 | .3 | .3 | .3 | .2 | .2 | .1 | .1 | .1 | .1 | .2 | .2 | .2 | .3 | .3 | .3 | .3 | .3 | .3 | .3 | .3 | .4 |
| SW PS,M.PV | .3 | .3 | .3 | .3 | .3 | .2 | .2 | .1 | .1 | .1 | .1 | .2 | .2 | .3 | .3 | .3 | .3 | .3 | .3 | .3 | .3 | .3 | .4 | .5 | .5 |
| TIMBALR IS | .2 | .3 | .3 | .3 | .3 | .3 | .2 | .2 | .1 | .1 | .1 | .1 | .1 | .2 | .2 | .2 | .3 | .3 | .3 | .2 | .2 | .3 | .3 | .3 | .4 |
| EUGENE IS | -.3 | -.4 | -.3 | -.1 | .1 | .3 | .5 | .6 | .6 | .4 | .2 | -.1 | -.4 | -.5 | -.5 | -.3 | -.1 | .1 | .3 | .5 | .5 | .5 | .4 | .2 | .1 |

* PRIMARY TIDE PREDICTION SITE - IF AVAILABLE

Figure 9.--An example of the computer output by SPLASH. The graph is the computed envelope of open coast high waters generated by hurricane Camille, 1969.

severe changes in horizontal depth contours on the shelf.

In figure 9, for the particular basin used, the peak surge varies by more than a factor of 3 on the last horizontal scale; this indicates the significance of local bathymetry in surge generation and hence the importance of landfall position.

Beneath the displayed graph, there is a printout of astronomical tide levels for selected stations for 12 hr before and 12 hr after the predicted time of landfall. The stations correspond to the cities listed on the graph above. Tides are predicted in feet above MSL.[16,17]

In principle, we could combine astronomical and meteorological tide for a total tide envelope. Although this appears to be a sensible procedure, such an envelope would be misleading. A display of this nature is meaningful only if we have an accurate knowledge of landfall in space and time and an accurate knowledge of the meteorological parameters; we just cannot forecast meteorological occurrences to the accuracy required. Neither would it be meaningful to display envelopes including highest and lowest expected values for a range of meteorological accuracy with time; the range between the two envelopes could be so large that the information would be almost useless.

The separate displays of surge envelope and tide forecasts allows the surge forecaster to correct for revisions in meteorology (i.e., he can update the surge prediction as his input data improves with time without constant rerunning of the program).

Hurricane Camille. This storm was discussed previously when we computed the peak surge only with precomputed nomograms. To illustrate the envelope of high water heights, with peak surge and its position on the coast, we compose the data deck of figure 13 (appendix 2) and let SPLASH print out the computer display of figure 9. In the figure, we have transferred the storm surge envelope to the inset of actual observed high water for comparison. At the time of landfall, the astronomical tide was miniscule; its diurnal range was less than a foot. For this reason, it is ignored.

The observed and computed curve seem to fit reasonably well except in the vicinity of peak surge. One could argue that the landfall position was slightly to the left of the computed position, that the storm size could be smaller, that observed values are not on the open coast, etc. We leave it to the reader to judge the results of the computed envelope.

---

[16] By "above MSL," we mean the tidal computations--for the rise and fall of the tide plus the annual variations of sea level--are with respect to a zero "datum"; thus, the computations can be added to any other datum. The datum used in the tide tables for the east and gulf coast stations is MLW (mean low water). The datum for contours on terrain charts is usually geodetic MSL; this does not always coincide with local MSL. For practical purposes, we can assume that the difference between geodetic and local MSL is very small; hence, our total tide--meteorological plus astronomical--can be compared directly with land contours for a measure of inland inundation.

[17] We use a tide program developed by Pore and Cummings (1967). The specific application here was developed by Lt. R. Garwood, NOAA Commissioned Corps.

Because Camille caused a record peak surge on the coast of the United States, it is interesting to know what the computed peak surge could be in surrounding coastal regions. The last horizontal line of figure 9 is a printout of potential peak surges on the coast if Camille had struck elsewhere on the coast and in the same relative way.

Hurricane Gracie. This particular storm is discussed to show the importance of the astronomical tide. The surge computed by SPLASH, tide predictions, and observed high-water marks are shown in figure 10. Meteorological data for this storm were supplied by the Hydrometeorology Branch, Water Management Information Division, NWS, NOAA.

The storm made landfall at Charleston, S.C., at 1100 LST when a low astronomical tide of -2.3 ft MSL existed in the landfall area. This means that the total peak surge was computed to be about 13.5 ft MSL (15.8 ft computed plus a low tide of -2.3 ft). The highest observed high-water mark was 11.9 ft 30 mi southwest of Charleston, but there may have been higher, unobserved surges to the northeast. The nearest tide gage to the landfall point was Charleston, and the highest surge of 5.9 ft occurred there at low tide; thus, computed surge becomes 9.3 -2.3, or 7.0 ft MSL. This agrees reasonably well with observed values in the Charleston area.

Consider now the observed values of 8+ ft in the Myrtle Beach, S.C., area. Note, particularly, that these values were measured by tide gages at 1700 hr, the time of high astronomical tide. Our computed values plus astronomical tide were about 4 ft lower than those observed. We will always have such problems at the ends of the envelope because:

1. Our model is designed to be most effective in the area of landfall and during landfall time.

2. Our computations, for economic and computational reasons, are terminated 3-9 hr after landfall, depending on storm speed. Hence, the ends are not completely representative.

3. The ends of the envelope, such as the area near Myrtle Beach in figure 10, are about 150 mi from the landfall point. Hence,

   a. curvilinear coastlines become significant, and

   b. the ends of the envelope are close to a fictitious lateral boundary in the basin where false wave reflections may play a part.

4. The surges at the ends of the envelope are sensitive to storm size R, a length difficult to observe.

The point is that high and low astronomical tides can superimpose separately on sections of the storm surge envelope.

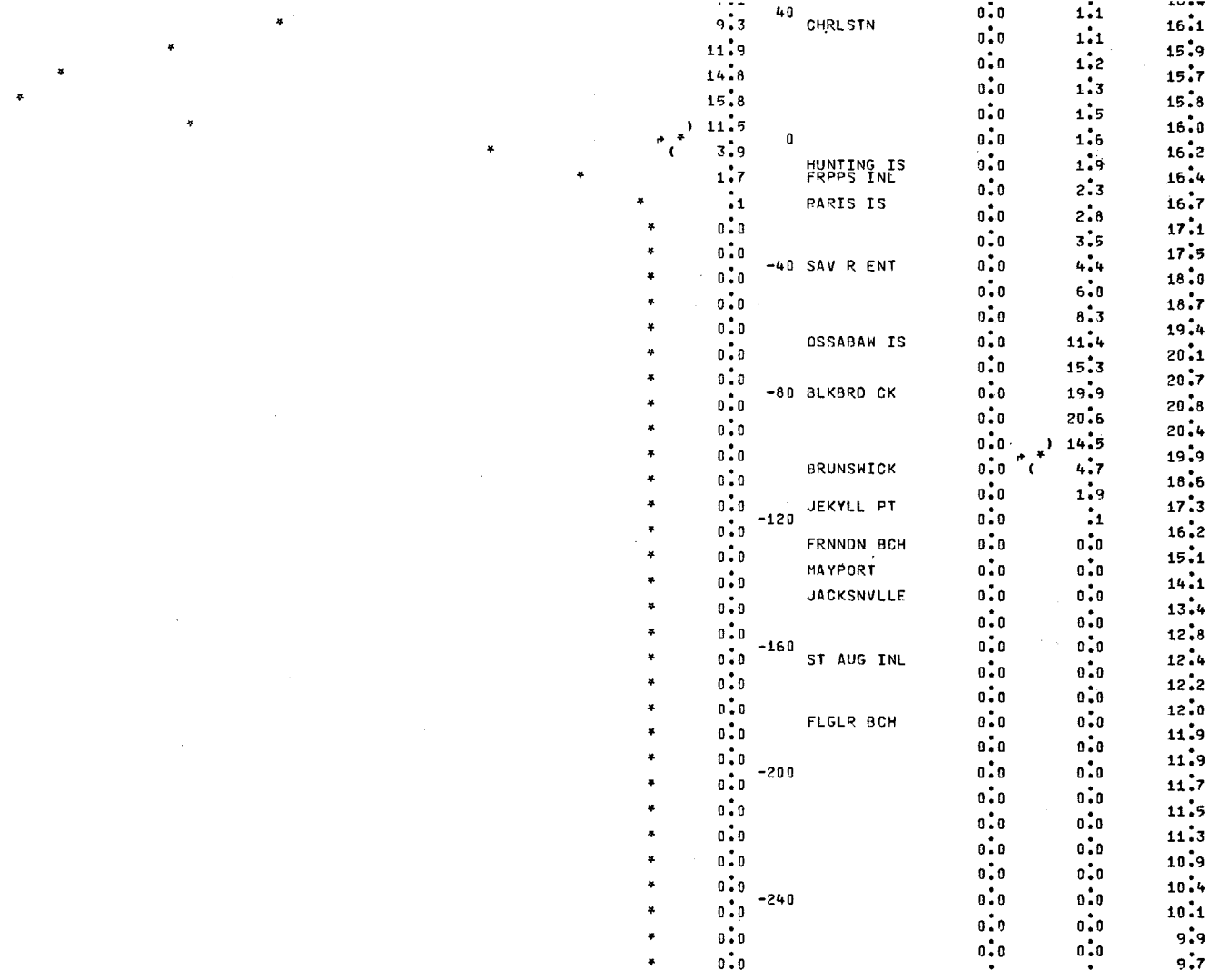


TIDE HEIGHTS ARE FT ABOVE MEAN SEA LEVEL.
HOURLY VALUES ARE PRINTED 12 HRS BEFORE TO
12 HRS AFTER ESTIMATED TIME OF LANDFALL.
ESTIMATED LANDFALL TIME 1100 LCL STD TIME, 29 SEP 1959 ESTIMATED TIME OF LANDFALL

| LCL STD TIME | 23 | 24 | 1 | 2 | 3 | 4 | 5 | 6 | 7 | 8 | 9 | 10 | 11 | 12 | 13 | 14 | 15 | 16 | 17 | 18 | 19 | 20 | 21 | 22 | 23 |
|---|---|---|---|---|---|---|---|---|---|---|---|---|---|---|---|---|---|---|---|---|---|---|---|---|---|
| NEW RV INL | -1.0 | -.7 | -.1 | .6 | 1.2 | 1.6 | 1.7 | 1.4 | .8 | .1 | -.6 | -1.0 | -1.1 | -.8 | -.3 | .5 | 1.2 | 1.8 | 2.0 | 1.8 | 1.2 | .4 | -.4 | -1.0 | -1.3 |
| CP FEAR | -1.6 | -.9 | .1 | 1.1 | 1.8 | 2.2 | 2.1 | 1.6 | .7 | -.3 | -1.3 | -1.9 | -1.9 | -1.3 | -.3 | .9 | 1.9 | 2.5 | 2.7 | 2.3 | 1.5 | .4 | -.7 | -1.7 | -2.0 |
| MYRTL BCH | -1.8 | -1.1 | .0 | 1.2 | 2.0 | 2.5 | 2.4 | 1.9 | .9 | -.3 | -1.4 | -2.2 | -2.2 | -1.6 | -.4 | .9 | 2.1 | 2.9 | 3.1 | 2.7 | 1.8 | .6 | -.8 | -1.9 | -2.3 |
| WNYH B ENT | -1.7 | -1.0 | .0 | 1.1 | 1.9 | 2.2 | 2.2 | 1.7 | .8 | -.3 | -1.3 | -1.9 | -2.0 | -1.4 | -.3 | .9 | 1.9 | 2.6 | 2.8 | 2.4 | 1.6 | .5 | -.7 | -1.7 | -2.1 |
| CHRLSTN * | -2.0 | -1.5 | -.5 | .7 | 1.7 | 2.4 | 2.6 | 2.2 | 1.4 | .3 | -1.0 | -1.9 | -2.3 | -2.0 | -1.0 | .4 | 1.7 | 2.6 | 3.1 | 3.0 | 2.3 | 1.2 | -.2 | -1.5 | -2.2 |
| FRPPS INL | -2.5 | -2.0 | -.8 | .7 | 2.0 | 2.9 | 3.1 | 2.7 | 1.7 | .4 | -1.0 | -2.2 | -2.8 | -2.5 | -1.4 | .2 | 1.8 | 3.1 | 3.7 | 3.5 | 2.7 | 1.4 | -.2 | -1.7 | -2.7 |
| SAV R ENT* | -2.8 | -2.4 | -1.2 | .5 | 2.0 | 3.1 | 3.5 | 3.1 | 2.2 | .7 | -.9 | -2.3 | -3.0 | -2.9 | -1.8 | -.1 | 1.7 | 3.2 | 4.0 | 4.0 | 3.2 | 1.8 | .1 | -1.6 | -2.8 |
| BLKBRD CK | -2.5 | -2.5 | -1.8 | -.4 | 1.2 | 2.5 | 3.2 | 3.2 | 2.6 | 1.4 | -.0 | -1.5 | -2.6 | -2.9 | -2.4 | -1.0 | .7 | 2.4 | 3.5 | 3.9 | 3.5 | 2.5 | 1.0 | -.7 | -2.1 |
| JEKYLL PT | -2.5 | -2.6 | -1.8 | -.3 | 1.3 | 2.6 | 3.2 | 3.2 | 2.6 | 1.4 | -.1 | -1.6 | -2.6 | -3.0 | -2.3 | -.9 | .8 | 2.5 | 3.6 | 3.9 | 3.5 | 2.4 | .9 | -.8 | -2.2 |
| MAYPORT * | -1.6 | -1.4 | -.7 | .2 | 1.2 | 2.1 | 2.5 | 2.5 | 1.9 | .9 | -.3 | -1.3 | -1.8 | -1.7 | -1.1 | -.1 | 1.1 | 2.1 | 2.8 | 3.0 | 2.6 | 1.6 | .4 | -.9 | -1.7 |
| ST AUG INL | -1.6 | -1.3 | -.6 | .4 | 1.4 | 2.2 | 2.6 | 2.4 | 1.7 | .6 | -.5 | -1.4 | -1.8 | -1.6 | -.9 | .1 | 1.3 | 2.3 | 2.9 | 3.0 | 2.4 | 1.4 | .1 | -1.0 | -1.8 |

* PRIMARY TIDE PREDICTION SITE - IF AVAILABLE

Figure 10.--Same as figure 9, except this is for hurricane Gracie, 1959

YOU HAVE SPECIFIED THE FOLLOWING STORM PARAMETERS

| | | |
|---|---|---|
| LANDFALL POINT IS | 36 MILES LEFT OF | CHARLESTON |
| THE STORM IS MOVING TO THE | NW AT 14.0 MPH | |
| THE PRESSURE DROP IS | 75 MBS. | |
| THE RADIUS OF MAXIMUM WIND IS | 12.0 STATUTE MILES | |
| THE MAXIMUM (SUSTAINED) WIND IS | 121.8 MPH | |

THE MAX WIND IS DERIVED FOR A (STATIONARY) STORM ON USING THE INPUT STORM PARAMETERS

IF YOU WANT TO UPDATE YOUR 75 MB PRESSURE DROP, USE THE FOLLOWING CORRECTION FACTORS ON THE COMPUTED SURGE VALUES

| UPDATED PRESSURE DROP | 65 | 67 | 69 | 71 | 73 | 75 | 77 | 79 | 81 | 83 | 85 |
|---|---|---|---|---|---|---|---|---|---|---|---|
| CORRECTION FACTOR | .86 | .89 | .91 | .94 | .97 | 1.00 | 1.03 | 1.05 | 1.08 | 1.12 | 1.13 |

STORM SURGE HEIGHTS (FEET)

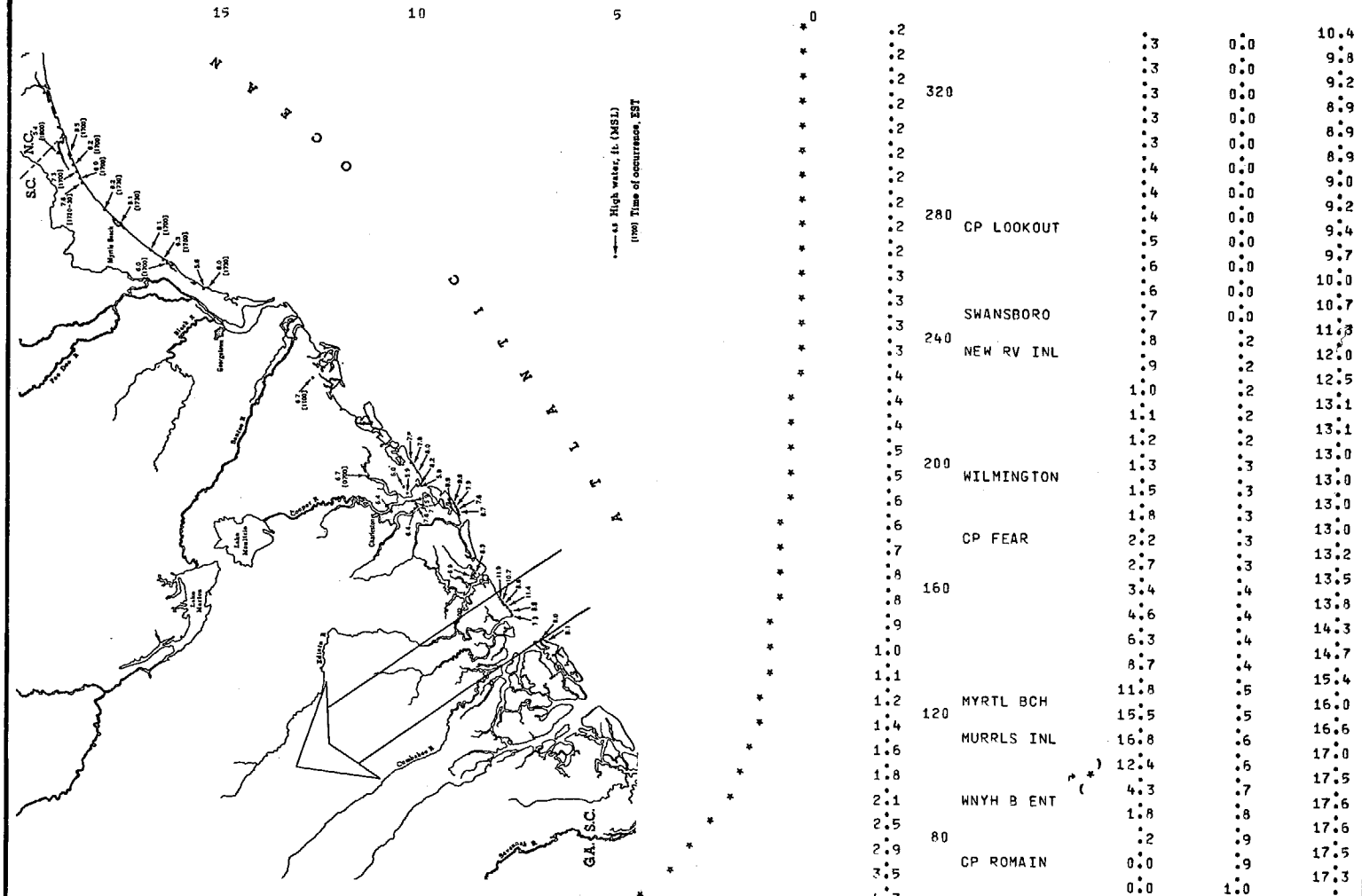

## 7. FURTHER COMMENTS AND CONCLUSIONS

Our dynamic storm surge model is only a first approximation for coastal surge phenomena. It is designed specifically for the open coast surge and assumes idealized conditions. These meteorological, geographical, and mathematical idealizations limit the model both for operations and research.

The meteorology for our storm model presupposes a moving steady-state storm; we describe it with parameters that are invariant in space and time (as the storm moves). It is a rather näive, simplistic model that needs improvement. Even so, a plethora of dynamic surge activity was extracted by using the storm model of this study. Operationally, it is pointless to use variable or changing storm parameters because currently they cannot be measured, much less forecast reliably. We can, however, easily incorporate variant parameters in the model for special studies, if so desired.

There are many interesting surge phenomena to be explored by means of parameters that vary in space or time. Meteorological observations, however, are just not available that describe wind and pressure changes on the entire sea surface while following the storm . There are some gross indications such as central pressure changes with time, forming or decaying double eye structures, etc.; but none of these are directly useful for description on the entire sea surface affected by the storm. It is tempting to extend the surge model by experimenting with variant storm parameters to see if the storm surge prediction would be significantly different. We are, however, in no position at this time to specify continuous dynamic changes in a storm as it moves within surrounding meteorological systems, across land surfaces, or across sea-surface temperature changes, or for more exotic situations such as cloud-seeding operations.

We point out that improvements in surge forecasting rest on improvements in meteorological data input. More sophisticated models for surge dynamics will not help operational forecasting if the meteorological data are not of the same quality. As an example, consider what a missed landfall point means for an unbroken versus a broken coastline:

1. On the unbroken coast, the surge envelope is merely translated to the new landfall point, with a relative amplitude correction for shoaling. The distortion of the envelope is not great unless the bathymetry about the new landfall point is drastically different.

2. On the broken coast--say, for a bay or estuary--the dynamics are entirely different, depending on which side of the broken coast the storm lands. It would not pay to make elaborate computations of the surge inside a bay or estuary for a storm forecast to move onto one side of the broken coast, but which in fact moves onto the opposite side.

For storms moving alongshore, no operational scheme has been designed for surge computations. We prefer to delay development at this time because the techniques required are much more complicated than for storms reaching land. Moreover, the results are quite sensitive to meteorological parameters (i.e., storm tracks are difficult to ascertain even in a climatological sense). These storms, moving at or nearly parallel to the coast, can generate specialized wave phenomena that, under certain circumstances, could be threatening if not

disastrous. The surge dynamics generated by these storms sometimes can be exceedingly complex compared with storms reaching land; however, such surges generally will be smaller in amplitude. Before going operational with these storms in the surge model, it is advisable for the surge forecaster to learn something about wave mechanics. He then can select storm parameters with a practiced eye on how they generate wave phenomena in a particular basin.

The surge model is neutral on the selection of storm parameters by the user; it makes no protest unless certain bounds are exceeded. This means that almost any number (for, say, the peak surge) can be computed depending upon meteorological input data. Because data from past storms at any selected point on the coast are sparse or even nonexistent, the way is open by any individual to supply processed data from climatology. We point out that the model is no better than the quality of the data used. The user should be careful and suspicious of broad, highly smoothed data from long stretches of space about the coastal area of interest; these may no longer be representative of meteorological conditions for particular problems under study.

## ACKNOWLEDGMENTS

I am deeply indebted to Dr. Albion Taylor for his many helpful suggestions, technical help in designing the computer program, and the many friendly hours of discussion on storm surge hydraulics. Appreciation is expressed to Lt. Roland Garwood, NOAA Commissioned Corps, who developed the astronomical tide program used in this paper. Special thanks are in order to Mr. Herman Perrotti for the graphic arts. Work on this project was supported in part by the National Science Foundation (NSF) under Grant AG-253, "NOAA Participation in the International Decade of Ocean Exploration (IDOE)."

## REFERENCES

Conner, W. C., Kraft, R. H., and Harris, D. Lee, "Empirical Methods for Forecasting the Maximum Storm Tide due to Hurricanes and Other Tropical Storms," Monthly Weather Review, Vol. 85, No. 4, Apr. 1957, pp. 113-116.

Cry, George W., "Tropical Cyclones of the North Atlantic Ocean: Tracks and Frequencies of Hurricanes and Tropical Storms, 1871-1963," Technical Paper No. 55, Weather Bureau, U.S. Dept. of Commerce, Washington, D.C., 1965, 148 pp.

Graham, Howard E., and Hudson, Georgina N., "Surface Winds Near the Center of Hurricanes (and other Cyclones)," National Hurricane Research Project Report No. 39, Weather Bureau, U.S. Dept. of Commerce, Washington, D.C., Sept. 1960, 200 pp. (see p. 123).

Harris, D. Lee, "Hurricane Audrey Storm Tide," National Hurricane Research Project Report No. 23, Weather Bureau, U.S. Dept. of Commerce, Washington, D.C., Oct. 1958, 19 pp.

Harris, D. Lee, "Characteristics of the Hurricane Storm Surge," Technical Paper No. 48, Weather Bureau, U.S. Dept. of Commerce, Washington, D.C., 1963, 139 pp.

Harris, D. Lee, "An Interim Hurricane Storm Surge Forecasting Guide," National Hurricane Research Project Report No. 32, Weather Bureau, U.S. Dept. of Commerce, Washington, D.C., Aug. 1959, 24 pp.

Holliday, Charles, "On the Maximum Sustained Winds Occurring in Atlantic Hurricanes," ESSA Technical Memorandum WBTM-SR-45, Weather Bureau Southern Region, Environmental Science Services Administration, U.S. Dept. of Commerce, Fort Worth, Tex., May 1969, 6 pp.

Hoover, Robert A., "Empirical Relationships of the Central Pressures in Hurricanes to the Maximum Surge and Storm Tide," Monthly Weather Review, Vol. 85, No. 5, May 1957, pp. 167-174.

Jelesnianski, Chester P., "Numerical Computations of Storm Surges With Bottom Stress," Monthly Weather Review, Vol. 95, No. 11, Nov. 1967, pp. 740-756.

Jelesnianski, Chester P. (Techniques Development Laboratory, National Oceanographic and Atmospheric Administration, U.S. Dept. of Commerce, Silver Spring, Md.), "Resonance Phenomena in Storm Surges" (unpublished manuscript), 1970, 30 pp.

Myers, Vance A., "Joint Probability Method of Tide Frequency Analysis Applied to Atlantic City and Long Beach Island, N.J.," ESSA Technical Memorandum WBTM HYDRO 11, Office of Hydrology, Weather Bureau, Environmental Science Services Administration, U.S. Dept. of Commerce, Silver Spring, Md., Apr. 1970, 109 pp.

Pore, N. A., and Cummings, R. A., "A FORTRAN Program for the Calculation of Hourly Values of Astronomical Tide and Time and Height of High and Low Water," ESSA Technical Memorandum WBTM TDL-6, Techniques Development Laboratory, Weather Bureau, Environmental Science Services Administration, U.S. Dept. of Commerce, Silver Spring, Md., Jan. 1967, 17 pp.

U.S. Army Corps of Engineers, "Report on Hurricane Betsy, 8-11 September 1965," Engineer District, New Orleans, La., Nov. 1965, 47 pp.

Weather Bureau, "Survey of Meteorological Factors Pertinent to Reduction of Loss of Life and Property in Hurricane Situations," National Hurricane Research Project Report No. 5, U.S. Dept. of Commerce, Washington, D.C., Mar. 1957, 87 pp.

## APPENDIX 1: EMPIRICAL AND NOMOGRAM SURGE MODELS

Connor et al. (1957) and Harris (1959) developed empirical statistical models to predict peak storm surges. The first of these papers was based on data from 30 hurricanes in the Gulf of Mexico. Because of the small size of the data sample, storm intensity was the only predictor considered. A correlation coefficient of 0.68 was obtained between observed and predicted surges when dependent data were used. In the second paper, data from 52 storms that occurred on both the Atlantic and gulf coasts were available for analysis. This time, it was possible to consider the slope of the Continental Shelf in a very crude way. The correlation coefficient was then increased to 0.75. The effect of storm size was found to be trivial. The data set was inadequate for a consideration of such dynamic effects as storm motion.

We want to see if the end product of our nomograms in the present paper does as well or better. To this end, we compare and correlate the observed peak surge values--adjusted for seasonal sea-level anomaly--against our peak surge approximations from nomograms.

A. Correlations Between Precomputed and Observed Surges

We have compared the observed peak surges reported for 43 of the 52 storms[18] used by Harris (1959) with predictions from the precomputed nomograms in this study (table 3). Seven of the tabulated storms have R greater than 50 mi, thus; they are not covered by the nomograms. Two entered New England where shoaling factors have not been developed. Missing in several of the tabulated storms are $P_{oo}$ and R; where this occurs, values of $P_{oo}$ = 1012 mb and R = 15 and 30 st.mi. have been assumed for the gulf and east coasts, respectively. For the vector storm motion parameters ($U_S$, $\theta$), we extracted from Cry (1965) the values[19] given while the storms were on the Continental Shelf.

In the first panel of figure 11, the peak observed surge is plotted against the predicted preliminary number $S_p$ derived from figure 1; thus, storm intensity and size of storm only are considered. The correlation coefficient, $\rho$, for the line of best fit for these data is 0.54 and loosely corresponds to the empirical model of Conner et al. (1957). For reference, a perfect forecast line slanted at 45° is drawn on each of the panels; this line could represent the conceptually ideal case when predictions and observations are identical; however, we view it as the line we want to approach with our issued forecasts. Comparing the difference in vertical or y values between the two lines gives a crude estimate for the reliability of our nomogram scheme.

The second panel gives a plot of the observed peak surge against a prediction by the nomogram method when the effects of storm intensity, storm size, and local bottom topography from figure 2 are considered. The prediction here is the product of $S_p \cdot F_{G,E}$. The correlation coefficient for the line of best fit with this data is 0.68. The panel corresponds loosely to the empirical model given by Harris (1959).

The third panel gives a plot of the observed peak surge against a prediction by the nomogram method when the effects of storm intensity, storm size, local bottom topography, and storm motion from figure 3 are considered. The prediction here is the product of $S_p \cdot F_{G,E} \cdot F_M$. The correlation coefficient for the line of best fit is 0.85.

Note that speed and direction of storm motion just might be correlated with the storm intensity and that both could be correlated with the location or landfall point of the storm. Although these secondary correlations may have

[18] Most of the meteorological data given by Harris comes from page 29 of the report by the Weather Bureau (1957). Note that $P_{oo}$ given by this reference does not always agree with historical weather maps; this is because meteorological parameters were derived quasi-empirically and random errors were allowed to accumulate in the ambient air pressure.

[19] The values extracted are somewhat subjective. This occurs because coast and track lines, which are curvilinear, are subjectively represented by straight lines.

Table 3.--Comparison of the observed peak surges reported for 43 of the 52 storms used by Harris (1959) with predictions from the precomputed nomograms in this study

| Storm | Date | Peak tide | $P_{oo}$ | $P_o$ | $\Delta P$ | R | $S_p$ | $F_{G,E}$ | $S_p \times F_{G,E}$ | $U_S$ | $\theta$ | $F_M$ | SS | h | Datum | SLA | h* |
|---|---|---|---|---|---|---|---|---|---|---|---|---|---|---|---|---|---|
| 1 | 2 Oct. 1893 | Mobile, Ala. | 1016 | 956 | 60 | 20 | 12.8 | 1.18 | 15.1 | 11 | 140 | 0.72 | 10.9 | 9.3 | MSL | M | 9.3 |
| 2 | 27 Sept. 1894 | Charleston, S. C. | 1012 | 986 | 26 | 30 | 5.6 | 1.17 | 6.6 | 12 | 120 | 0.79 | 5.2 | 5.3 | AN | M | 5.3 |
| 3 | 8 Sept. 1900 | Galveston, Tex. | 1009 | 936 | 73 | 16 | 15.1 | 1.02 | 15.4 | 13 | 080 | 0.98 | 15.1 | 14.6 | MSL | M | 14.6 |
| 4 | 14 Aug. 1901 | Mobile, Ala. | 1021 | 973 | 48 | 38 | 10.5 | 0.79 | 8.3 | 8 | 090 | 0.82 | 6.8 | 7.4 | MSL | M | 7.4 |
| 5 | 27 Sept. 1906 | Ft. Barrancas, Fla. | 1018 | 965 | 53 | 75 | radius greater than 50 mi, storm out of range | | | | | | | | | | |
| 6 | 21 July 1909 | Galveston, Tex. | 1025 | 959 | 66 | 22 | 14.2 | 1.02 | 14.5 | 9 | 060 | 0.80 | 11.6 | 10.0 | MSL | M | 10.0 |
| 7 | 20 Sept. 1909 | Timbalier I. , La. | 1026 | 980 | 46 | 102 | radius greater than 50 mi, storm out of range | | | | | | | | | | |
| 8 | 18 Oct. 1910 | Everglades, Fla. | 1008 | 959 | 49 | 55 | radius greater than 50 mi, storm out of range | | | | | | | | | | |
| 9 | 13 Sept. 1912 | Mobile, Ala. | 1012 | 993 | 19 | 15 | 3.9 | 0.79 | 3.1 | 13 | 080 | 0.96 | 3.0 | 4.4 | MSL | M | 4.4 |
| 10 | 16 Aug. 1915 | High I., Tex. | 1001 | 953 | 48 | 37 | 10.3 | 1.09 | 11.2 | 16 | 080 | 1.05 | 11.8 | 13.9 | MSL | M | 13.9 |
| 11 | 29 Sept. 1915 | Grand Isle, La. | 1021 | 944 | 77 | 34 | 17.0 | 0.76 | 12.9 | 12 | 100 | 0.87 | 11.2 | 9.0 | MSL | M | 9.0 |
| 12 | 5 July 1916 | Ft. Morgan, Ala. | 1017 | 961 | 56 | 57 | radius greater than 50 mi, storm out of range | | | | | | | | | | |
| 13 | 18 Oct. 1916 | Pensacola, Fla. | 1023 | 974 | 49 | 50 | 9.5 | 0.61 | 5.8 | 15 | 110 | 0.90 | 5.2 | 3.0 | MSL | M | 3.0 |
| 14 | 28 Sept. 1917 | Ft. Barrancas, Fla. | 1012 | 964 | 48 | 37 | 10.5 | 0.59 | 6.2 | 12 | 090 | 0.93 | 5.8 | 7.1 | MSL | M | 7.1 |
| 15 | 9 Sept. 1919 | Key West, Fla. | 1007 | 929 | 78 | 17 | 16.3 | 0.53 | 8.6 | 9 | 040 | 0.85 | 7.3 | 6.6 | MSL | 0.1 | 6.5 |
| 16 | 25 Oct. 1921 | Punta Rassa, Fla. | 1002 | 958 | 44 | 21 | 9.4 | 1.28 | 12.0 | 12 | 070 | 0.90 | 10.8 | 11.0 | MSL | 0.1 | 10.9 |
| 17 | 26 Aug. 1926 | Timbalier I. , La. | 1028 | 959 | 69 | 31 | 15.9 | 0.75 | 11.9 | 9 | 070 | 0.83 | 9.9 | 10.0 | MSL | 0.2 | 9.8 |
| 18 | 18 Sept. 1926 | Miami Beach, Fla. | 1016 | 934 | 82 | 28 | 18.3 | 0.70 | 12.8 | 13 | 100 | 0.91 | 11.7 | 10.5 | MSL | 0.1 | 10.4 |
| 19 | 20 Sept. 1926 | Pensacola, Fla. | 1020 | 955 | 65 | 24 | 14.5 | 0.61 | 8.8 | 9 | 060 | 0.81 | 7.2 | 9.4 | MSL | 0.4 | 9.0 |
| 20 | 16 Sept. 1928 | West Palm Beach, Fla. | 1029 | 935 | 94 | 32 | 22.2 | 0.47 | 10.4 | 15 | 120 | 0.86 | 9.0 | 9.8 | AN | 0.1 | 9.7 |
| 21 | 28 Sept. 1929 | Key Largo, Fla | 1019 | 953 | 66 | 32 | 15.2 | 0.54 | 8.2 | 12 | 070 | 0.89 | 7.3 | 8.8 | MSL | 0.0 | 8.8 |
| 22 | 23 Aug. 1933 | Hampton Roads, Va. | 998 | 970 | 28 | 62 | radius greater than 50 mi, storm out of range | | | | | | | | | | |
| 23 | 7 Sept. 1933 | Brownsville, Tex. | 1024 | 949 | 75 | 35 | 17.2 | 0.64 | 11.0 | 11 | 090 | 0.90 | 9.9 | 13.0 | MSL | M | 13.0 |
| 24 | 25 July 1934 | Galveston, Tex. | 1012 | 975 | 37 | 15 | 7.3 | 1.02 | 7.4 | 13 | 040 | 0.91 | 6.8 | 5.9 | MSL | M | 5.9 |
| 25 | 4 Nov. 1935 | Miami Beach, Fla. | 1012 | 973 | 39 | 30 | 8.7 | 0.70 | 6.1 | 18 | 070 | 1.09 | 6.6 | 9.3 | MSL | 0.3 | 9.0 |
| 26 | 31 July 1936 | Panama City, Fla. | 1016 | 964 | 52 | 22 | 11.3 | 0.60 | 6.8 | 10 | 060 | 0.82 | 5.6 | 6.0 | MSL | 0.0 | 6.0 |
| 27 | 21 Sept. 1938 | Moriches, N.Y. | 1000 | 943 | 57 | 58 | radius greater than 50 mi, storm out of range | | | | | | | | | | |
| 28 | 7 Aug. 1940 | Colcasieu Pass, La. | 1008 | 974 | 34 | 13 | 6.4 | 1.16 | 7.4 | 5 | 030 | 0.71 | 5.3 | 4.8 | MSL | 0.1 | 5.3 |
| 29 | 11 Aug. 1940 | Beaufort, S. C. | 1017 | 975 | 42 | 30 | 9.3 | 1.15 | 10.7 | 8 | 060 | 0.75 | 8.0 | 8.5 | AN | 0.5 | 8.0 |
| 30 | 23 Sept. 1941 | Sargent, Tex. | 1004 | 959 | 45 | 24 | 9.9 | 0.88 | 8.7 | 13 | 110 | 0.88 | 7.7 | 9.9 | MSL | 1.4 | 8.5 |
| 31 | 7 Oct. 1941 | St. Marks, Fla. | 1022 | 981 | 41 | 21 | 8.4 | 1.32 | 11.1 | 13 | 100 | 0.91 | 10.1 | 6.4 | MSL | 0.3 | 6.1 |
| 32 | 30 Aug. 1942 | Matagorda, Tex. | 1004 | 951 | 53 | 21 | 11.5 | 0.79 | 9.1 | 16 | 080 | 1.04 | 9.5 | 14.8 | MSL | 0.8 | 14.0 |
| 33 | 27 July 1943 | Galveston, Tex. | 1017 | 975 | 42 | 19 | 8.6 | 1.02 | 8.8 | 4 | 060 | 0.66 | 5.8 | 4.0 | MSL | 0.4 | 3.6 |
| 34 | 14 Sept. 1944 | Newport, R.I. | 992 | 959 | 36 | 26 | shoaling factor unavailable | | | | | | | | | | |
| 35 | 19 Oct. 1944 | Naples, Fla. | 1004 | 962 | 42 | 39 | 8.6 | 9.24 | 10.7 | 16 | 060 | 1.00 | 10.7 | 11.0 | MSL | 0.4 | 10.6 |
| 36 | 20 Oct. 1944 | Charleston, Fla. | 1012 | 991 | 21 | 30 | 4.2 | 1.17 | 4.9 | 16 | 140 | 0.81 | 4.0 | 4.4 | AN | 0.4 | 4.0 |
| 37 | 27 Aug. 1945 | Matagorda, Tex. | 1020 | 968 | 52 | 21 | 11.3 | 0.79 | 8.9 | 7 | 140 | 0.69 | 6.2 | 7.3 | AN | 0.9 | 6.4 |
| 38 | 24 Aug. 1947 | Sabine Pass, La. | 1012 | 992 | 20 | 15 | 3.9 | 1.11 | 4.3 | 4 | 080 | 0.68 | 2.9 | 3.6 | MSL | 1.1 | 2.5 |
| 39 | 17 Aug. 1947 | Hillsboro Beach, Fla. | 1010 | 940 | 70 | 22 | 15.3 | 0.47 | 7.2 | 11 | 080 | 0.89 | 6.4 | 9.8 | MSL | 0.3 | 9.5 |
| 40 | 19 Sept. 1947 | Biloxi, Miss. | 1006 | 968 | 38 | 32 | 8.3 | 1.20 | 10.0 | 23 | 040 | 1.12 | 11.2 | 11.1 | MSL | 0.2 | 10.9 |
| 41 | 15 Oct. 1947 | Quarantine Sta., Ga. | 1004 | 968 | 36 | 15 | 7.1 | 1.22 | 8.7 | 10 | 060 | 0.81 | 7.0 | 6.5 | AN | 0.7 | 5.8 |
| 42 | 4 Sept. 1948 | Biloxi, Miss. | 1012 | 987 | 25 | 15 | 4.9 | 1.20 | 5.9 | 14 | 110 | 0.88 | 5.2 | 5.6 | MSL | 0.5 | 5.1 |
| 43 | 26 Aug. 1949 | New Jupiter In., Fla. | 1020 | 954 | 66 | 25 | 14.5 | 0.48 | 7.0 | 14 | 130 | 0.77 | 5.4 | 4.2 | MSL | 0.1 | 4.1 |
| 44 | 4 Oct. 1949 | Freeport, Tex. | 1020 | 978 | 42 | 32 | 9.4 | 0.89 | 8.4 | 20 | 110 | 1.05 | 8.8 | 10.4 | AN | 1.4 | 9.0 |
| 45 | 30 Aug. 1950 | Pensacola, Fla. | 1006 | 979 | 27 | 24 | 5.6 | 0.61 | 3.4 | 18 | 080 | 1.10 | 3.8 | 5.5 | MSL | 0.4 | 5.1 |
| 46 | 5 Sept. 1950 | St. Petersburg, Fla. | 1012 | 958 | 54 | 15 | 10.8 | 1.28 | 13.8 | 10 | 270 | 0.50 | 6.9 | 7.2 | MSL | 0.9 | 6.3 |
| 47 | 31 Aug. 1954 | Sakonnet Pt., R.I. | 1012 | 961 | 51 | 30 | shoaling factor unavailable | | | | | | | | | | |
| 48 | 15 Oct. 1954 | South Port, N.C. | 993 | 937 | 56 | 16 | 11.5 | 0.95 | 10.9 | 26 | 120 | 1.14 | 12.5 | 12.7 | AN | 0.2 | 12.8 |
| 49 | 17 Aug. 1955 | Holden Beach, N.C. | 1012 | 986 | 26 | 30 | 5.5 | 1.00 | 5.5 | 13 | 090 | 0.96 | 5.3 | 6.0 | AN | 0.6 | 5.4 |
| 50 | 19 Sept. 1955 | Morehead City, N.C. | 1012 | 966 | 46 | 58 | radius greater than 50 mi, storm out of range | | | | | | | | | | |
| 51 | 24 Sept. 1956 | Laguna Beach, Fla. | 1012 | 974 | 38 | 30 | 8.5 | 0.59 | 5.0 | 13 | 100 | 0.94 | 4.7 | 7.4 | AN | 0.3 | 7.1 |
| 52 | 27 June 1957 | Calcasieu Pass, La. | 1006 | 947 | 59 | 22 | 13.0 | 1.17 | 15.2 | 16 | 080 | 1.04 | 15.8 | 13.9 | AN | 1.4 | 12.5 |

$P_{oo}$ Outside ambient pressure (in mb)
$P_o$ Central pressure (in mb)
$\Delta P$ $P_{oo} - P_o$
R Radius of maximum winds (in st.mi.)
$S_p$ Preliminary number for peak surge
$F_{G,E}$ Shoaling factor for gulf or east coast
$U_S$ Speed of storm (in mph)
M Missing

$U_S$ Speed of storm (in mph)
$\theta$ Direction of storm traverse relative to coast
$F_M$ Correction factor for vector storm motion
SS Computed storm surge ($S_p \cdot F_{G,E} \cdot F_M$)
h Observed high tide (in ft)
SLA Seasonal sea-level anomaly (in ft)
h* High tide adjusted for SLA
AN Above normal

contributed to the skill obtained with the purely empirical models, they were deliberately rejected in the construction of our nomograms from dynamic calculations. This is presumed to be the major reason why the correlation coefficients of the first two panels in figure 11 are smaller than those obtained in the corresponding empirical models.

The data in table 3 leave much to be desired. Although some of the peak surge values came from tide-gage records, most were from post-storm surveys

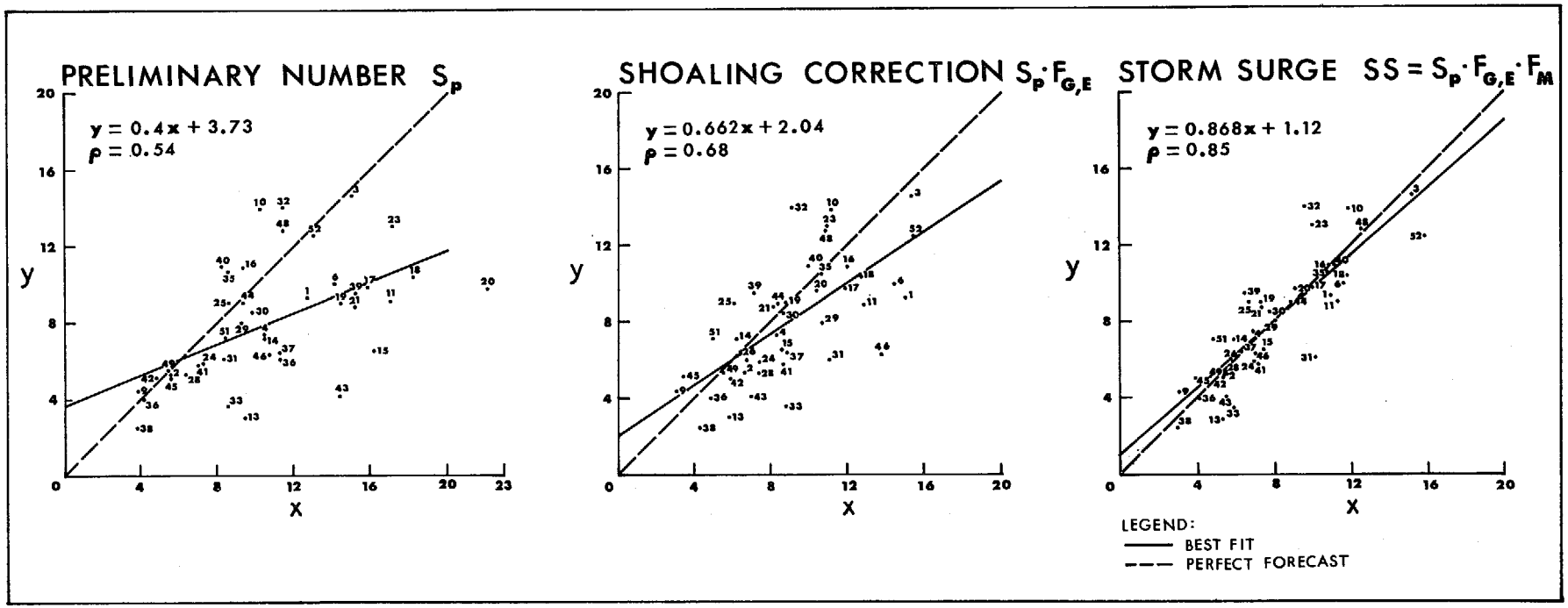


Figure 11.--Correlation between the nomogram-computed x coordinate and the observed y coordinate peak surges. See table 3 for the data used. The number on the data points represents the storm number in table 3. The first panel correlates the preliminary number $S_p$ derived from the nomogram of figure 1. The second panel corrects for local bathymetry. The third panel further corrects for the vector storm motion and gives the final product SS the computed storm surge.

Table 4.--Mean square differences between nomogram-computed and reported peak surges

| | Considering size and intensity of storm only | Including a correction for local topography | Including a correction for speed and direction of storm motion |
|---|---|---|---|
| Departure from perfect forecast line; no statistical adjustment | 4.56 ft | 2.74 ft | 1.68 ft |
| Departure from least-squares(best fit) regression line | 2.62 ft | 2.30 ft | 1.63 ft |

of high water marks. In general, it was not possible to take the stage of the astronomical tide into consideration in evaluating the effects of the storm. It is unlikely that the actual peak surge would coincide with one of the small number of high water marks measured. It is likely that purely local factors have contributed to most of the high water marks listed; and it is unlikely that the storm parameters $P_o$ and $P_{oo}$ and the speed and direction of the storm were sufficiently correct in all cases, particularly for the earlier storms. It should be noted that the only fitting between the predictions and the reported peak surges permitted in this evaluation are the regression coefficients and line of best fit shown in figure 11.

## B. Composite Nomogram and Statistical Model

We want to combine our predictions from nomograms with available statistics to arrive at a possible better peak surge estimate. To this end, let the abscissa x in figure 11 represent a forecast from our nomograms and let the ordinate y represent the forecast issued. If we use nomograms only for our forecast, then the perfect forecast line must be used; however, there are times when we can correct the nomogram prediction with available statistics. To combine statistics with our nomograms, we should use the line of best fit (fig. 11) to issue a forecast.

To show how the two lines in figure 11 differ, we will consider the mean square differences between the reported peak surge values and those predicted by:

1. The nomogram scheme only (i.e., using the perfect forecast line).

2. The best fit regression line.

These are given in table 4. It is seen that the least-squares regression line gives no significant improvement over our nomogram scheme when all of the meteorological data are used.

One might suspect that individual computations with the dynamic model (instead of nomograms) fitted directly to the local bathymetry and to the individual storm parameters might give even smaller average differences between reported and computed values.

When the approximate nature of the parameters assigned to many of the early storms is considered, it appears that the individual calculations could be justified for only a very few of the early storms. Individualized computer runs with the dynamic model are currently being made for all hurricanes entering the mainland of the United States.

## Using the Composite Model for Initial Planning Purposes

When a tropical storm is first discovered, we have either very limited or no meteorological information. With time, the information dribbles in--in the form of observations, forecasts, climatology, or even speculation. Nevertheless, for incomplete meteorological information, the composite model can be useful. What we have in mind here is to use whatever information is available for the best possible forecast.

Initially, we know a storm exists, confirmed, say, by satellite observations. This in itself is not sufficient information to proceed with the nomogram computations for storm surges. We might, however, ascertain information indirectly from cloud pictures, climatology, or experience. Generally though, we must be content to wait for in-situ observations, such as ship reports and dropsondes.

The first--and most useful--piece of information is the pressure drop; it allows us to determine from our first nomogram the preliminary number[20] $S_p$. At this stage, the history of the storm is unknown; and we do not know the landfall point or storm motion. Therefore, the number $S_p$ is the best we can do with our nomograms.[21] We can, however, revise this crude number with available statistics. This is done with the line of best fit on the first panel of figure 11; we enter with $S_p$ on the x axis and issue a revised preliminary number from the y axis through the line of best fit. The revised number, a general number for the entire coast, is the best that can be done until more information becomes available.

Suppose, for the next piece of information, we determine (or assume) a land fall point; we then appraise surges locally (rather than generally) on the open coast. This is done by multiplying the preliminary number $S_p$ with the shoaling factor of our second nomogram and forming the product of $S_p \cdot F_{G,E}$. We enter this product on the x axis of the second panel of figure 11 and use the line of best fit to issue a locally revised preliminary number for our prediction. This number is the best we can do until the last piece of information (storm motion) becomes available.

Suppose we now ascertain the last piece of information (storm motion). We then formulate the final product of $S_p \cdot F_{G,E} \cdot F_M$, where $F_M$ is the motion factor from our third nomogram. This new product, call it SS, is entered on the x

[20] R can be chosen arbitrarily. The peak surge is not unduly sensitive to this parameter.

[21] We remind you that these nomograms were designed only for the gulf and east coasts.

axis of the third panel of figure 11; in this case, the issued forecast is just as good whether we use the line of best fit or the perfect forecast line (i.e., we need not revise the number SS to issue a forecast). When we have sufficient information to enter the third panel, available statistics no longer help to improve our forecast.

## APPENDIX 2: SPLASH

Our purpose here is not to give a detailed description of the program, but to describe a simple procedure to run it with minimal effort. This procedure can be used by part-time limited-experience programmers such as operational weather forecasters. Access to a computer, at least by terminal drop, is assumed.

### A. Mechanics of Running the Program

The approach adopted here is to store SPLASH onto tape; the program is called for an operational run by a small program of only a few cards, followed by a data deck of pertinent meteorological parameters. The tape is divided into three files composed of:

1. A program deck in binary.

2. Thirty basins and their geography, each basin separated by an EOR card.[22]

3. A program deck in FORTRAN (formula translator).

The program is run with the binary deck; the FORTRAN deck is present in case a listing of the program is desired.

The tape program is written for the NOAA CDC 6600 computer; it is <u>not</u> compatible with the software of other computers. To call and run the taped program, one needs a small program of several cards. This is shown in figure 12.

The first card of the small program, JOB card, is self-explanatory. For a given storm, it usually takes about 2 min of CP or central processing time to run the program. For exceptionally large or slow-moving storms, it may take 4 min of CP time. The T400 on the card represents 400 octal seconds (or about 4 min decimal) needed for CP.

The second card requests the program tape. MXXXXX is used to designate the tape number. The tape is physically located at the CDC Computer Center, FOB-4, Suitland, Md.; it is administered by NHC, the National Hurricane Center at Miami, Fla., where numbers are assigned to the five X's. The tape will be revised as time goes by; to run it, the user will have to make periodic arrangements with the NHC.

---

[22] A CDC 6600 EOR (end of record) card is one with the 7, 8, and 9 holes punched in column 1.

```
          SMALL PROGRAM DECK TO CALL PROGRAM TAPE (SINGLE JOB)

JOBNO,CM77000,T400,TP1.
REQUEST,TAPE1,HI,E.      USE MXXXXX
REWIND,TAPE1.
RFL,15000.
CKLBL(TAPE1,MXXXXX)
REWIND TAPE1.
COPYBF(TAPE1,SPLASH)
COPYBF(TAPE1,TAPE9)
RETURN,TAPE1.
RFL,77000.
SPLASH.
EXIT.
RETURN TAPE1.
7-8-9          (END OF RECORD CARD)
          (DATA DECK, SEE FIGURE 13)
6-7-8-9        (END OF FILE CARD)


          OBTAINING A FORTRAN LISTING WITH A JOB RUN (MULTI JOBS)

JOBNO,CM77000,T400,TP1.
REQUEST,TAPE1,HI,E.      USE MXXXXX
REWIND,TAPE1.
RFL,15000.
CKLBL(TAPE1,MXXXXX)
REWIND TAPE1.
COPYBF(TAPE1,SPLASH)
COPYBF(TAPE1,TAPE9)
COPYBF(TAPE1,OLDPL)
RETURN,TAPE1.
RFL,77000.
SPLASH.
SPLASH.
   .
   .
   .
SPLASH.
RFL,60000.                 DELETE THESE FIVE CARDS IF
UPDATE(P,F,L=0)            A LISTING OF THE FORTRAN
COPYSBF(COMPILE,OUTPUT)    PROGRAM IS NOT DESIRED
EXIT.
RETURN TAPE1.
7-8-9
          (FIRST DATA DECK)
7-8-9
          (SECOND DATA DECK)
7-8-9
   .
   .
   .
7-8-9
          (LAST DATA DECK)
7-8-9
6-7-8-9
```

Figure 12.--Program decks for use with SPLASH

The small program deck in figure 12 will run only one job. If one desires to run several consecutive jobs (say, for other landfall points on either side of predicted landfall), then insert the card

| | |
|---|---|
| SPLASH. | 2d job |
| SPLASH. | 3d job |

after SPLASH and repeat the last card for any following jobs. Of course, meteorological data--the data deck--must be supplied separately for each job; data decks will be discussed in the next topic. Also, TXXXX in the job card must be revised to accommodate a longer run time. If a listing of the FORTRAN program is also desired, the procedure shown in figure 12 can be used.

## B. Meteorological Data Deck for the Program

To predict storm surges by computer, one must describe the tropical storm prior to landfall. This is done with simple meteorological parameters that can be prepunched on data cards. Forecasters at weather stations are best equipped to handle this; for this reason, the program is designed for their use.

The data deck for the program consists of two title cards (followed by six storm data cards) and is terminated by four time cards for astronomical tide. The two title cards are self-explanatory. The form and style of the storm and tide data cards require some explanation; they represent the parameters given in figure 13.

The first two storm data cards give landfall position. Although latitude and longitude would seem likely coordinates for this position, we follow common usage instead and refer landfall position relative to a geographical landmark or station. Stations used in the program are listed in table 2. The geographical locations of the stations are shown in figure 5; they are approximately 100 mi apart.

For the first storm data card, use the nearest station to landfall. The station letters begin on the first space of the card, never exceed 10 spaces, and are punched exactly as printed in table 2, spaces and all; any spaces beyond the 10th space can be used for comments. We use an A10 format here.

For the second storm data card, use the distance (in st.mi.) for the landfall point lying to the right or left of the station as viewed from sea by one facing land. Use a negative sign only if landfall is left of the station. Use the first five spaces of the card; any spaces beyond can be used for comments. We use an I5 format[23] here. Note that the first two storm data cards are used by the machine to position local two-dimensional bathymetry in the basin and to orientate the coast relative to north.

For the third storm data card, use the pressure drop (in mb) while the storm traverses the Continental Shelf. Note, $10 \leq \Delta P \leq 140$ in the program. Use the first five spaces of the data card; any spaces beyond can be used for comments. We use an I5 format here.

For the fourth storm data card, use the mean compass direction (meteorological sense) in which the storm will traverse the Continental Shelf just prior to landfall. The admissible directions in the program are 16 points boxed on the compass. They are in letters, not degrees. Use the first three spaces of the card, always ending on the third space; any spaces beyond can be used for comments. We use an A3 format here.

For the fifth storm data card, use the average storm speed (in mi/hr) during traverse over the Continental Shelf just prior to landfall. Note, $6.0 \leq \text{speed} \leq 60.0$ in the program. Use the first five spaces of the card; any spaces beyond can be used for comments. The speed can be in decimals if desired. We use an F5.1 format here.

For the sixth storm data card, use the average storm size (in st.mi.) during its traverse over the Continental Shelf. The storm size is R, the radius of

---

[23] For all I5 formats, punch the number right justified. That is, the units digit is in the fifth space, the 10's digit in the fourth space, etc. Otherwise, the number will not be read in properly; and the computer will supply a zero for each blank space (e.g., 10 mi/hr is punched ^^^10, where '^' means a blank space.

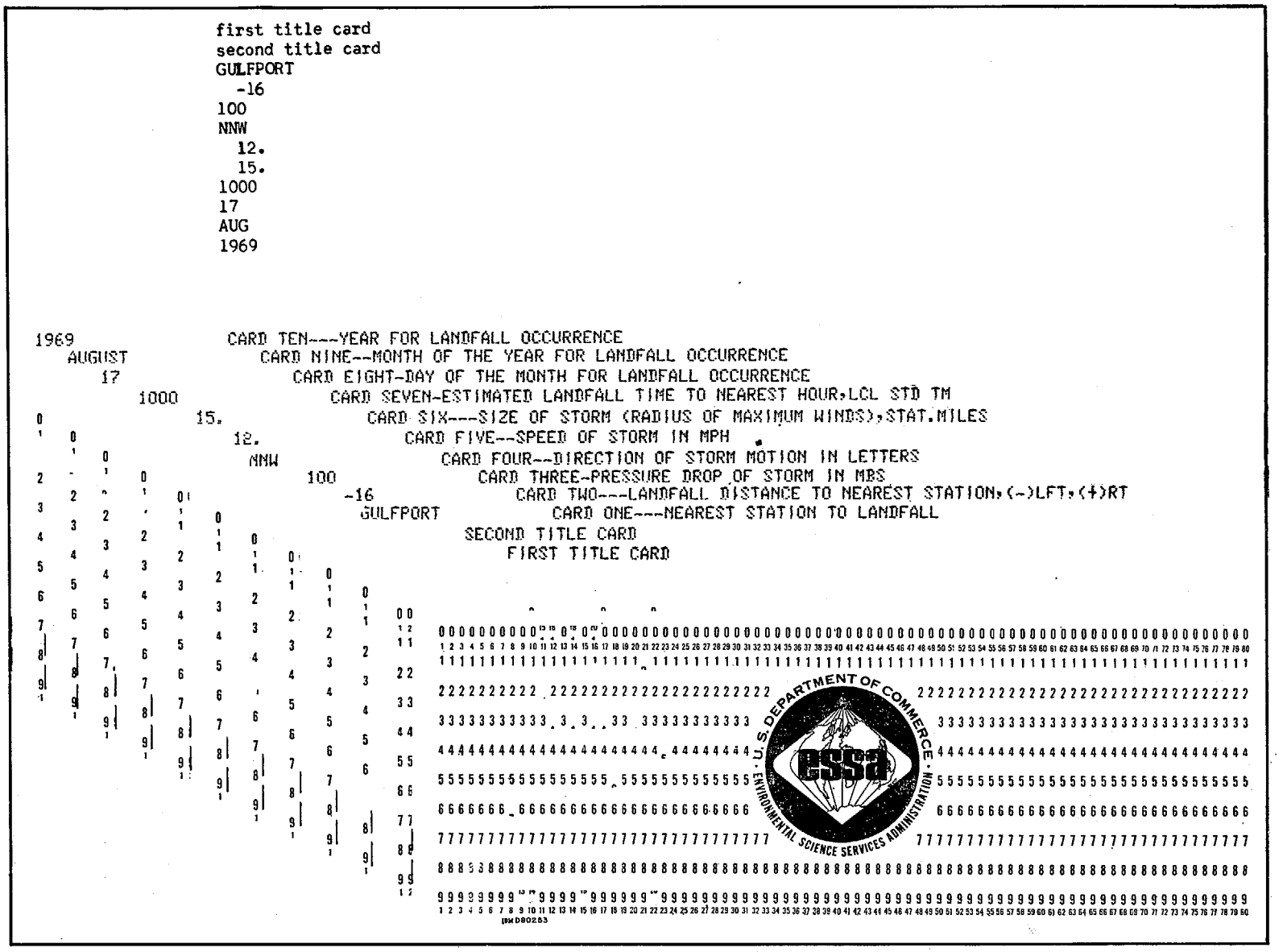


Figure 13.--An example of a data deck. It is inserted immediately after the small program deck of figure 12.

maximum winds. Note, $10.0 \leq R \leq 60.0$ in the program.[24] Use the first five spaces of the card; any spaces beyond can be used for comments. The size can be in decimals if desired. We use an F5.1 format here.

The program constraints for storm data cards 3, 5, and 6 can be changed, if so desired, only by updating the taped FORTRAN deck through UPDATE procedures; we do not discuss this operation here and refer the user to CDC manuals.

The next four data cards are optional; they are used for astronomical tide predictions. If not presented in the data deck, the program will ignore tide computations.

For the seventh data card, use the nearest integer hour of landfall, from 0100 to 2400. Use the first four spaces of the card and let the last two spaces be zeros; any spaces beyond can be used for comments. We use an I4 format here.

For the eighth data card, use the day of landfall, from day 01 to day 31. Use the first two spaces of the card; any spaces beyond can be used for comments. We use an I2 format here.

For the ninth data card, use the month of landfall. Use the first three letters of the month in the first three spaces of the data card; any spaces beyond can be used for comments, including the complete spelling of the month. We use an A3 format here.

For the 10th data card, use the year of landfall. The years can lie between 1900 and 1999 for past-present-future predictions of astronomical tide. Use the first four spaces of the data card; any spaces beyond can be used for comments. We use the I4 format here.

An example of a punched data deck is shown in figure 13; the deck is set in the small program as shown in figure 12. The cards must be in sequence. If N jobs are to be executed, then set N data decks in the small program; separate each data deck with an EOR card. Behind the last data deck, insert an end of file (EOF) card.[25]

It is suggested that data cards be prepunched to reflect all ranges of meteorological and time parameters. In this way, the user can assemble cards that best describe tropical storms and their landfall times without punching errors.

## APPENDIX 3: SOME DO'S, DON'TS, AND APPLICATIONS WHEN FORECASTING STORM SURGES

The operational computer output developed in this study is a useful tool. As such, it should be considered only an aid for the prediction of, or planning for, storm surges. It is not a substitute for experience and judgment. We advise that there are inherent weaknesses in the dynamic model used here and there will always be uncertainties in the meteorological input data;

---

[24] It is doubtful if such a large-sized storm as 60 mi can be adequately represented by our model.

[25] A CDC 6600 EOR card is one with the 7, 8, and 9 holes punched in column 1. An EOF card has the 6, 7, 8, and 9 holes punched.

the user must judiciously apply his knowledge to shore up and buttress these inadequacies.

It is a fact that forecasters will extrapolate the limited range of any model well beyond physical constraints. Therefore, we want to discuss and develop some criteria for evaluating the output surge computations. We will want to adjust the computer product, at least qualitatively, for inherent weaknesses and uncertainties.

The discussions in this appendix will be mostly qualitative, even speculative; they are intended to guide and warn the user engaged in storm surge prediction. First, meteorological parameters and their relative importance will be considered. Next, we will consider coastal geographical features and how they alter the surge locally.

## A. Meteorological Parameters

When tropical storms threaten a coast, much interest is centered on the value of the meteorologically forecast maximum wind--fastest mile (Holliday 1969). This physical number is readily assimilated by communities, planners, and others. The tendency then is to use it as a direct measure for potential damage.

For storm surge generation, we must strongly resist the temptation to use the forecast maximum wind[26] as a direct measure of the peak surge. Instead, we should pay strict attention to parameters directly accessible and amenable to measurements.

### Pressure Drop

What we need paramountly to concentrate on is the pressure drop of the storm. The peak surge value varies almost linearly with the pressure drop; and this value is quasi-conservative with respect to storm size.

1. Errors in pressure drop ($\delta p$) are significant only when significant in comparison to the pressure drop $\Delta p$ (i.e., the ratio between $\delta p$ and $\Delta p$ is the deciding factor).

   a. For small pressure drops, we must have quite accurate readings (forecasts) of the storm's central pressure.

   b. For large pressure drops, such as that of hurricane Camille, we can afford more error in the central pressure readings.

2. The relative error of pressure drop is a measure of the corresponding relative error of peak surge value.

3. If the storm is deepening while traversing the Continental Shelf, use the central pressure at the time of landfall.

   a. If the central pressure deepens dramatically with time, there will be some overshooting of surge amplitudes. This is why the lowest central

[26] We can use an average maximum wind around the circle of radius R. This is significantly smaller than the fastest mile wind.

pressure at the time of landfall is used rather than a mean central pressure.

4. If the storm is filling while traversing the Continental Shelf, use the mean central pressure of the storm during traverse.

a. If the central pressure fills dramatically with time, there will be a lag in surge amplitude adjustments. This is why we use a higher central pressure than that expected at landfall.

Size of Storms

Of secondary importance for peak surge values is the storm size. Although large variations in storm size (say, by a factor of 2) generally have only a mild effect on the peak surge value, we should not be too cavalier about choosing its value. We point out that larger storm cause surges along a larger length of coast; also, the potential for inland inundation is greater.

Direction of Storm Motion Relative to the Coast

For operational and illustrative convenience, let the coast and storm track be straight lines. There are two extreme positions of these lines with respect to each other, either normal (a landfall storm) or parallel (along shore-moving storm). Each extreme has two particular orientations:

1. Landfall storms.

   a. Storm moves from sea to land.

   b. Storm moves from land to sea (exiting storm).

2. Storms moving alongshore.

   a. Storms moving up the coast.

   b. Storms moving down the coast.

For the particular orientations within each extreme, the surge profile and peak surge value are significantly different.

The varieties of dynamical behavior for each extreme are vastly different, all dependent on the meteorological parameters and basin used. For storm tracks between the two extremes, the storm surge profile undergoes transitional changes.

Herein lies one advantage for direct machine computations with the dynamic model; dynamic effects for particular situations are directly incorporated in the computations.

<u>Storms Reaching Land</u>. Storms reaching land, traveling <u>near normal</u> to the coast, generate surge profiles that grow with time. The position of the highest surge on the profile remains nearly stationary; eventually, it reaches peak surge amplitude at approximately the time of landfall. Exiting storms (i.e., storms traveling from land to sea) follow a similar pattern, but with a smaller peak surge.

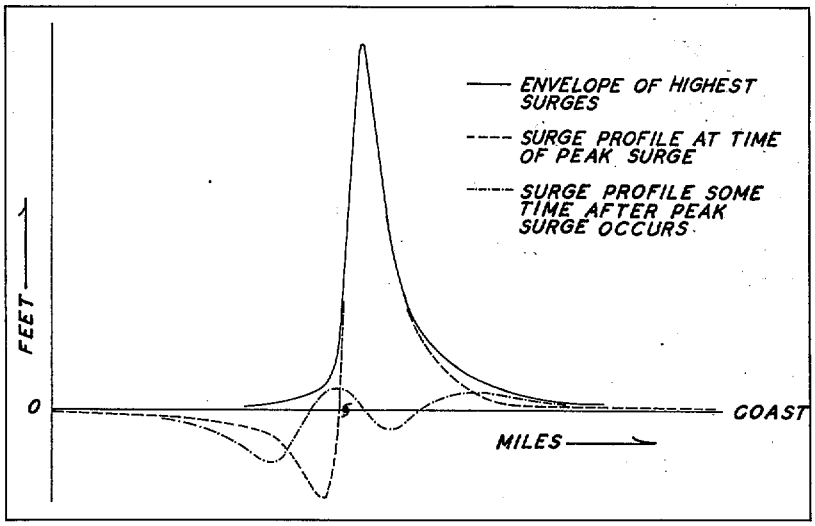


Figure 14.--Envelope of coastal high water heights for coastal surge profiles

For conceptual purposes, we can view the coastal surge profile at the time of peak surge as a string that is held or plucked by the storm at or near the time of landfall. Of course, things are not quite so simple as the mechanics of a plucked string; but the illustration is informative. An example of such a profile is shown in figure 14. Note that there are negative surges to the left of the storm; furthermore, these negative values are larger for exiting storms. With passage of the storm, we now view the profile as a released string that forms two waves moving to the right and left, respectively. The form and speed of propagation of these two waves depend on the input meteorological parameters and basin used. To portray a convenient end product of this phenomena, we consider the envelope of all high water heights on the coast and call it the storm surge envelope. The form of the envelope along the coast represents the observed high water heights, without respect to time of occurrence.

If the storm travels other than normal to the coast, then the highest surge on the profile prior to landfall is no longer stationary in space; the highest surge moves along the coast following the storm on its track. This continues until peak surge occurs. The net result is that the envelope of high water heights is elongated along the component of track direction on the coast; this can mean a long length of coast will be affected by surges for storms that move nearly parallel to the coast. Only one end of the surge envelope can become elongated, but only for storms traveling nearly parallel to the coast.

Storms Moving Alongshore. These storms generate interesting assortments of complicated wave phenomena. It is not easy to summarize all these wave phenomena for ordinary forecasting.

One problem in forecasting these surges, possibly insurmountable at this time, is the lack of advance knowledge of meteorological parameters. Not only do we need to know the track of the storm--which can easily exceed 500 mi--but also the possible or probable large variations of storm parameters along the track with time. The art of weather forecasting has not yet advanced to the point where these parameters can be predicted reliably for 2 or 3 days in advance.

Storms moving alongshore generally cause significantly smaller surges than storms reaching land. An exception could occur with storms traveling at particular speeds in particular basins so as to generate a resonance condition (Jelesnianski 1970); the direction of travel must be down the coast, that is $\theta$ is 0° (see fig. 3 for orientation). Fortunately, this case will almost never occur except possibly with a storm traveling northward along the west coast of Florida. Generally, storms move alongshore only on the eastern seaboard.

The portrayal of storm surge profiles for storms moving alongshore will be deferred to a later paper.

Landfall Position and Storm Track

For operational procedures, such as evacuation decisions, we must know the length of coast threatened with significant surges. This length is roughly the diameter of the storm where surges are greater than one-half the peak surge value The 24-hr-forecast error in landfall position is about the same order of magnitude; hence, it is desirable to ascertain the landfall point as precisely as possible. Another reason for precise positioning is the effect of local bathymetry on surges; more will be said about this later.

In connection with landfall point, we need to appraise how vector storm motion affects surges. For the following, use figure 3 as applicable.

1. Storms traveling from sea to land generate larger surges than those traveling from land to sea.

a. The opposite holds for negative surges (an observer positioned at sea while facing land will find negative surges to the left of landfall at the time of peak surge).

2. For storms traveling <u>near normal</u> to the coast, small variations in storm speed can affect peak surge values significantly. The opposite is true for small variations in storm direction.

a. For storms traveling from sea to land, the peak surge increases with increased speed until a critical speed is reached. Critical speed is rarely reached; exceptions can occur with very small storms or on wide and shallow shelves.

b. For storms traveling from land to sea, the peak surge decreases with increasing storm speed. There is no critical speed.

3. For storms traveling <u>nearly parallel</u> to the coast, small variations in storm direction can affect peak surge values significantly. The opposite is for small variations in storm speed. Here, we need to know the storm track and landfall rather precisely.

4. When determining the storm track, use the direction of the mean vector motion of the storm during its traverse across the shelf.

## B. Geographical Features of Basins and Their Coastlines

The dynamic model assumes an ideal basin (shown in fig. 15A). Its properties are:

1. A straight unbroken coastline.

2. Land elevations rising vertically on the coast, with

   a. finite sea depths ($D_o$) on the coast.

3. A wide shallow shelf where the width is greater than R, but of the same order of magnitude.

Real basins do not satisfy all of these properties; but for basins along the United States and attendant coasts, conditions do not deviate too much from the model basin. What we will need to do is to consider the ratios of several scale sizes for particular basins against storm size R. These ratios will help to guide us in selecting a range of nonidealism that is tolerable in our storm surge model. In what follows, only the sense (not magnitude) of corrective action on our open coast surge forecasts will be discussed for natural basins.

### Unbroken Coastlines

At this point, we consider coastlines that are unbroken by bays, estuaries, and inlets. No natural coastline is straight; all are curvilinear to some extent. In figure 15B, we show a curvilinear coast with a radius of curvature $R_C$ at the landfall point. For operational convenience when faced with the problem of determining $R_C$, we suggest a visual estimate by first drawing a circle of radius R for the storm, tangent to the coast at the landfall point. If the direction of $R_C$ is toward the sea, as shown in the figure, we call the coast "concave downward." If the direction of $R_C$ is toward land because of opposite curvature, we call the coast "concave upward."

We now formulate some criteria of a qualitative nature for a range of applicability with the storm surge model.

1. If $R_C \gg R$, then consider the coast a straight line and do not correct for curvature. (The symbol $\gg$ can be interpreted as an order of magnitude greater.)

2. If $R_C > R$, then the curvature of the coast can have a significant effect on surges. (The symbol $>$ can be interpreted as greater than, but of the same order of magnitude.

   a. If $R_C$ is concave downward, the generated surge will be greater than on a straight line coast.

   b. If $R_C$ is concave upward, the generated surge will be smaller than on a straight line coast.

# Do Not Scan

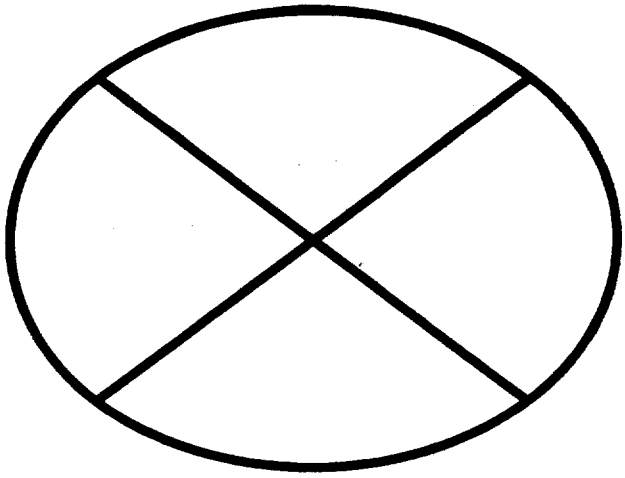

## Reprep-Insert Do Not Scan Document Here

**Document ID:** Figure #16

~~between~~ Map / Chart

**Page #:** between pg 40/41

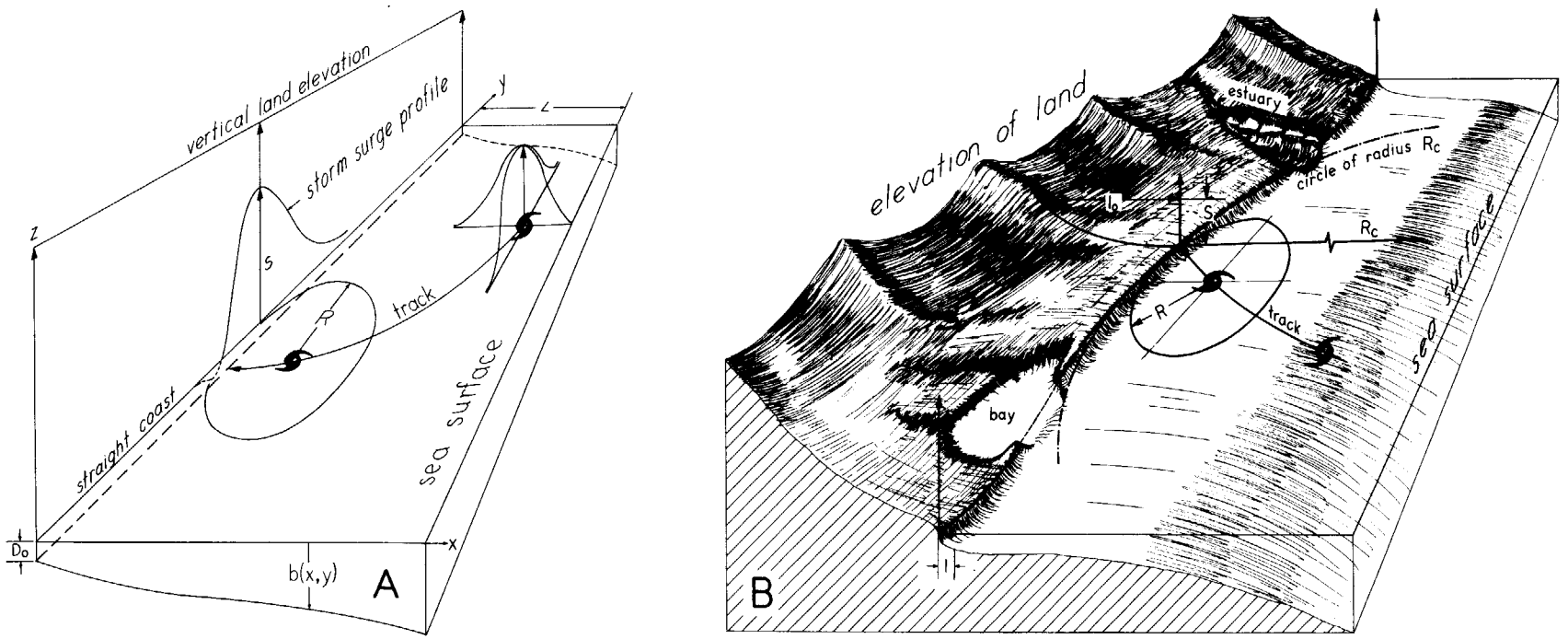


Figure 15.--(A) idealized model of the open coast surge generated by a traveling tropical storm reaching land. The area immediately adjacent to the straight line coast is represented by a vertical wall. (B) same as (A), except this is for a more realistic basin. The coast is curvilinear and borken by bays and estuaries; the areas immediately adjacent to the coast form a slanted surface rather than a vertical wall.

3. If $R_C < R$, then we are out of range for the model. Some examples are:

a. Capes that prominently mark a change in or interrupt the coastal trend and on which the curvature is concave upward.

b. Corner points that prominently mark the meeting of two separate coasts at an angle (e.g., Long Island and the mainland; Florida Keys and Florida) and on which the curvature is concave downward.

4. If $R_C \ll R$, but the surrounding coast also is equally irregular, then we still consider the coastline as being nearly straight. What we have in mind here is a ragged coastline where each localized feature is much smaller in scale than the storm. We realize that ragged coastlines will generate surge profiles that are ragged in appearance.

Broken Coastlines

Coastlines are broken by bays, estuaries, deltas, and inlets. There are no precise definitions for these coastal indentations. We will consider only indentations with widths or lengths of the same magnitude as our storm sizes.

Bays. A bay is somewhat oval shaped with its longest axis more or less parallel to the coast. A bay differs from a closed lake in that part of its boundary, the mouth, is exposed to the sea; at most, there is a barrier island on the seaward side of the bay. The following may be applicable.

1. For a bay to the right (as viewed from the sea) of an exiting storm or one reaching land, the surge on the landward sides of the bay will be larger than surges computed for the open coast. By "sides," we also mean portions of the lateral sides of the bay.

2. For a bay to the left of an exiting storm or one reaching land, the surge on the seaward sides of the bay (not including the mouth) will be larger than that on the landward sides and that computed by the model for the open coast.

3. The left lateral side of the bay will have higher surges than those along the right lateral side.

The surges at the mouth of the bay may be much smaller than those computed by the numerical model for the unbroken coast.

Hurricane Carla. For an example of the bay effect, see figure 16 that gives surges for hurricane Carla, 1961, an exceptionally large and slow-moving storm.[27] The inset gives observed surges for comparison with the computed surge envelope. Available tide gage readings (Harris 1958) show a remarkably long duration for the higher surges. Since landfall occurred near the time of high astronomical tide, peak meteorological and astronomical tides were nearly simultaneous. The astronomical tide was about 0.5+ ft

[27] Meteorological data were subjectively determined from the Monthly Weather Review, bulletins, advisories, etc.

# Do Not Scan

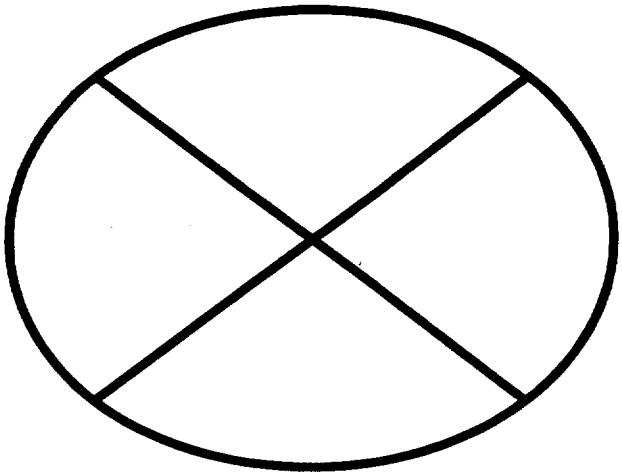

## Reprep-Insert Do Not Scan Document Here

**Document ID:** FIGURE 17
MAP & CHART

**Page #:**

above MSL; if we add this to the computed surges from just to the left of landfall to Galveston, then the computed surges agree with observed values to almost the nearest foot along the unbroken open coast. We do not make such comparisons for the ends of the envelope, especially to the left of landfall, where coastal boundaries curve significantly.

On the inset, to the left of landfall, all bays appear to have larger surges on the seaward sides. Because of the lack of open coast surge measurements and dynamic effects of coastal curvature, we cannot make comparisons with the model envelope. To the right of landfall, all bays appear to have larger surges on the landward sides. The ratio of landward to seaward surges appears to be greater in Galveston than Matagorda Bay; we suggest this may be attributed in part to the more rapidly changing driving forces about the storm's core as it crossed Matagorda Bay.

The barrier islands about Matagorda Bay were inundated, and there are no surge measurements to compare with the computed envelope. If we assume that the maximum surge on the model envelope is representative for the open coast, then the bay effect increased the maximum surge. The highest measured surge of 22 ft appears to be an extreme local effect; the next highest still-water, high-water mark is 19 ft. This is not too far from the computed maximum surge of 15.9 ft (astronomical tide[28] added) on the model envelope.

The surges in Sabine Lake do not appear to have any preferred areas for higher surges. Note that the lake has no significant exposure to the sea.

Estuaries. An estuary is usually rather long and narrow, somewhat like a canal, with its axis more or less normal to the coast. Usually, a large river discharges into the head of an estuary at the end opposite its mouth; several smaller rivers also may discharge into the sides. On marine charts, estuaries often are listed or named as bays. Estuarine effects are less known than bay effects; at this stage, we are nearly helpless in specifying surge characteristics for estuaries. Exceptions are specialized studies for idealized canals that do not directly concern us here. We speculate that estuarine effects are as follows.

1. If the axis of an estuary is smaller than R, then estuarine effects are similar to bay effects, but possibly smaller in ratio. Mobile Bay on the Alabama coast is an example of such an estuary.

2. If the axis length is larger than the storm's diameter, then the situation is indeed complicated. The surge will depend in part on vector storm motion relative to the axis. We are in no position to list all possible phenomena, but we can speculate qualitatively and warn for the following:

a. If the axis is to the right (as viewed from the sea) of an exiting storm or one reaching land and if the track parallels the axis, then conditions could be ripe to generate a substantial surge. By "ripe," we mean a critical storm speed for a given estuary. However, we do not as yet know the critical speed for particular estuaries.

[28] High astronomical tide occurred 2 to 3 hr after landfall; high storm surge changed slightly during this period because of slow storm motion. No attempt was made to correct for SLA, the seasonal sea-level anomoly.

b. If the axis is to the left of an exiting storm or one reaching land and if the track parallels the axis, then the surges at the mouth and head of the estuary are reversed (i.e., the mouth will have positive surges while the head will have negative ones).

c. If the storm track crosses the axis, there will be many variations of the surge in space and time within the estuary.

We remark that the surge at the mouth of an estuary may be much smaller than that computed by the model for the unbroken coast.

Inlets. An inlet is a short, narrow waterway connecting an inland feature (e.g., bay, lagoon, or inner coast) with the sea. What we have in mind here is a long barrier island parallel to the coast and broken by inlets; the island has high vertical dunes, and there is a narrow sound or intracoastal waterway between the coast and island. An example of this is along the northeast coast of Florida. A storm reaching land on this coast may generate surges that do not overtop the dunes, but can and do enter the inlets. Currently, we are in no position to discuss the dynamics of this situation or to give operational rules for forecasting. Presumably, if the inlet length is larger than R, then the surge can be expected to reach the segment of the coast inland from the inlet. We can even ignore a sound much smaller in width than R. We do not know, however, how far the surge moves into the sound on either side of the inlet.

For large-scale sounds with inlets such as Long Island Sound between Long Island and Connecticut, we are completely helpless. These features are similar in many respects to the estuary.

Deltas. A delta is an alluvial deposit surrounding the mouth of a river or inlet. Deltas have various shapes and sizes. An extreme example is the triangular shaped delta on the coast of East Pakistan. It consists of several rivers, inlets, and islands juxtaposed about the coast. For effects of deltas on the open coast surge, we admit to almost complete helplessness in specifying any characteristics.

Our main concern in the United States is the Mississippi Delta that has a digitate shape extending into the sea; its length is the same magnitude as storm sizes. In part, it resembles a cape. The coast on either side of the delta is confused and choatic with bays and many lakes not too far inland. All these irregularities destroy the reliability of the open coast computations in a delta area. We cannot formulate firm guides for the surge forecaster; reference to past storms and subjective comparison of observed or computed surges might be helpful here. We warn, however, that vector storm motions in the future may be different from those observed in the past, which may radically alter the dynamics of surge generation about the delta.

Hurricane Betsy. For an example of a storm striking in this area, consider hurricane Betsy, 1965. Figure 17 gives computed and observed surges for this storm; meteorological data were subjectively extracted from such sources as the Monthly Weather Review, bulletins, and advisories. Note that the observed surges about the mouth of the delta are significantly smaller than those at the head of the delta; this could be attributed to the steepness of the Continental Shelf at the mouth and its shallowness on either side of the

delta. In our model, we ignore the delta and substitute shallow water to connect the shelves on either side of delta; we also ignore the islands between Chandeleur Sound and the gulf and between Mississippi Sound and the gulf.

Except for the delta itself, the model shows some skill. The observed and computed surges show fair agreement on the open coast at Grand Isle, Pt. Pleasant, Gulfport, Biloxi, etc. The highest computed surges, off Hopedale on the open coast, are for an area devoid of observations; thus, it may be that we do not know how high the actual surges[29] were for this storm.

We remark on a subtle interplay (in this geographical area) that could be important. Notice that peak surge was computed to lie 52 mi to the right of the landfall point, a distance significantly larger than R = 32 mi for the storm. This seeming discrepancy in placement of peak surge relative to the landfall point is caused by severe horizontal changes of the ocean depth contours to the right of the landfall point. For an explanation of this dynamic phenomena, see figure 8. Had the same storm made landfall several miles to the right of the observed landfall, then the shoaling phenomena could have produced more dramatic peak surge; this is shown in the last horizontal line of figure 17 where the potential peak surge on the coast is given. Note that there can be sizeable differences between potential and computed peak surge heights for any particular point on the coast. The message here is that, in geographical areas with severe horizontal changes in the ocean depth contours, the peak surge and its placement on the coast are sensitive not only to the landfall point but also to the size of the storm.

## C. Inundation

A storm moving across a sloping continental shelf builds a mound of water that eventually impinges on the coast. Momentum then forces the mound of water to charge up the coast, a situation we call "runup" (Harris 1963). Runup is a complicated nonlinear phenomena; but for long gravity waves such as storm surges, we can make approximations. Consider the vertical and horizontal components of runup; these are S and $l_o$ is shown in figure 15B where S is the open coast surge and $l_o$ is length of inundation normal to the coast. Along $l_o$, the heights of the inland surges vary in a complicated fashion in space and time; these variations are not considered in the model.

In the model, a vertical[30] wall is used to represent the landward terrain. How well does a vertical wall represent the near-horizontal terrain? Well, it does not exactly, but it does approximately. We use this approximation when $l_o$ is small compared to some length normal to the coast. For convenience,

[29] The terrain in question is very shallow; inundation effects may have decreased the open coast surge. See the next topic for a description of inundation effects.

[30] The inland slope of the terrain from the coast usually is about two orders of magnitude greater than the slope of the surge normal to the coast; this means that the long gravity wave (storm surge) sees the inland terrain approximately as a vertical wall, even though the inland slope may be numerically quite small.

measure $l_o$ as the inland distance where the land contour (elevation) and computed peak surge are equal. The following may be applicable.

1. If $l_o < R$ along the open coast, then computed surges are a good representation for the open coast surge.

2. If $l_o > R$, then our computed surges are larger than the natural open coast surges.

Our model tells us nothing about inland inundation. We cannot say analytically whether the surges decrease or increase inland. However, this situation becomes critical only when item 2 occurs. In practice, it is usually assumed that surges decrease inland.[31]

Hurricane Audrey. For an example of inundation effects, consider hurricane Audrey, 1957. This was a storm of ordinary intensity compared to Carla or Camille. Figure 18 shows a comparison of computed and observed surges for this storm.[32] Note that the inland area, about and to the east of landfall, is very flat except for several low-lying ridges paralleling the coast; in fact, one must proceed 20 to 30 mi inland before the terrain rises to as much as 10 ft. This flat terrain virtually guarantees that $l_o > R$; exceptions would occur only with weak storms.

The observed surges for this storm were extensively studied by Harris (1958); we use his data in the following discussion. To compare observed and computed surges, we note that landfall occurred at high tide of about 0.5 ft; Harris (1958) gives a seasonal sea-level anomaly of 1.4 ft in the area affected by this storm. Hence for comparisons, we will have to add about 2 ft to the computed surge.

The nearest observation, with respect to position of computed peak surge, showed 12.1 ft just west of Cameron; this was not a strict measurement but rather a reconstruction of partial data from a tide gage destroyed by the storm. We note a gap in observations just east of Cameron where highest tide may have occurred.[33] The computed surge envelope (plus a 1- to 2-ft correction) gives 1 to 5 ft higher surges than observations inland from the open coast; this is for the core of the envelope between Sabine and Southwest Passes. Overall, the observed surges tended to decrease inland; but there are exceptions, especially about Calcasieu Lake. We remark that inland surges, at

[31] We would emphasize that observed, inland, high-water marks are not water above terrain but rather above MSL. As an example, a 15-ft high-water mark on terrain 10 ft above MSL means that there is 5 ft of water above the terrain in question. Sometimes rain will flood pockets of land in high terrain. This may give the illusion of runup from a very high open coast surge. Similarly, rivers overflowing their banks should not be confused with runup of the surge.

[32] Meteorological data for this storm were extracted from Graham and Hudson (1960). These data were accepted as is.

[33] The landfall position and storm size are best estimates from available meteorological data, formulation, etc. (see footnote 32). Thus, there is some uncertainty as to the position of the computed peak surge.

# Do Not Scan

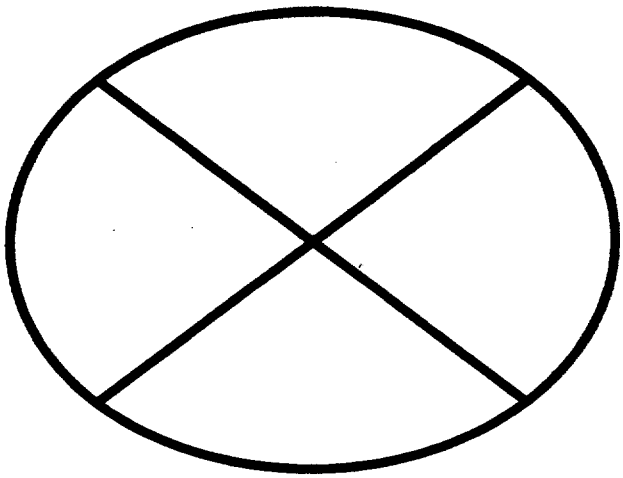

## Reprep-Insert Do Not Scan Document Here

**Document ID:** Figure 18
Map & Chart

**Page #:**

distances comparable to storm size R, may and no doubt are significantly smaller than the open coast surge.

For another example of the inundation phenomena, consider the large-sized storm Carla, 1961 (fig. 12). Here, $l_o < R$; and the computed surges plus the astronomical tides are representative for the observed open coast surge. The observed surge heights do not always decrease inland, and they do not follow any easily discernible pattern.

In both examples, the effects of curvilinear coasts, bays, lakes, etc., follow patterns similar to those discussed in previous topics.

Wave setup. When a wave breaks on a coast, the chaotic mass of water runs up the coast; this occurs because the water mass has energy to dispose. After runup, the mass of water should flow back to the sea but is prevented from completing the action by succeeding breaking waves. After some time, an equilibrium pattern is formed in which the mean water level inland and seaward from the coast is other than normal. This situation is called "wave setup"; this can be negative or positive in the area influenced by breaking waves.

Our empirical knowledge of wave setup comes mostly from laboratory wave tanks under idealized conditions, not from natural basins during hurricane conditions. Note especially that wave setup is an equilibrium state with short gravity waves breaking periodically.

The storm surge is a long gravity wave. It too runs up the coast but does not break. The surge also runs down the coast after the storm passes; but because there are no following long waves, it cannot form wave setup. During runup, the elevated surge can act as a pathway for short-gravity, breaking waves (e.g., surf and swell) farther inland; but in almost all cases, the breaking activity does not extend much beyond the normal coast. One should remember that the slope of inland terrain is considerably different from the seaward slope in the wave-breaking zone. A large surge occurring in flat terrain will inundate the land for several miles inland; it is possible that the wind pattern in a slow-moving storm may form short-gravity, breaking waves in the inundation area; but it takes time to do this, sometimes a lot of time. We cannot assume a priori that wave setup, in the positive sense, automatically takes place; nor can we assume it acts more favorably in a given area merely because the surge measurements are higher than expected. The phenomena is just too complex to give operational rules at this time; we need an extensive and exhaustive study on generation of short-gravity, breaking waves during surge inundation before speaking authoritatively about wave setup.

We do not consider wave setup in our computations because it is a nonlinear phenomena not too well understood during transient surge states. It is possible that wave setup is partially, and indirectly, accounted for in our model through the drag coefficient in our wind stress formulation. The surge forecaster should have sound physical reasons before applying corrections for wave setup onto surge computations.

## D. Continental Shelf Width, Depths, and Grid Spacing

In the dynamic model, the computational grid spacing must be small enough to detect a passing storm of given size. The spacing serves equally well for computing the generated surge wave because its length[34] under the storm is directly related to storm size. A 4-mi grid spacing is sufficient for most storms reaching land; exceptions would be for storms with $R < 10$ mi. For economic and operational reasons, the entire ocean cannot be used in the model; therefore, we use only a segment of the Continental Shelf. This necessitates the introduction of open boundaries in our truncated basin. We must also contend with the wide variations of shelf width along the United States and improvise when shelves are not compatible with the surge model.

We require a shelf width in the model. On the basis of empirical computations, this width must be at least of size R.[35] For operational convenience, we set our shelf width as 72 mi, larger than any R used in the model. The coastal surge computations are not sensitive to the exact width of the shelf edge, even if it is much wider than 72 mi.

It is difficult to define precisely the edge of the Continental Shelf. The depths on the edges vary considerably along the United States. For the constant invariant grid size used in the model, we dare not allow the depths to become too large because of economic and computational limits; hence, we must improvise. From results with empirical computations, we find that the coastal storm surge is not sensitive to depths greater than 300 ft; accordingly, no depth on the Continental Shelf is allowed to exceed this limit. What is so magical about 300 ft? Well, our model incorporates some of Ekman's concepts in linking driving forces with momentum. This means that the transfer of momentum downward into the sea by wind stress is constrained to an Ekman depth[36] of about 300 ft. Also, for a time invariant surface stress, it takes more than a day for momentum to reach equilibrium at the Ekman depth; but the storm traverses the Continental Shelf in less than a day, except possibly for exceptionally slow storms.

---

[34] An exception could be resonant or trapped waves a short distance from land (Jelesnianski 1970).

[35] The computed coastal surge begins to vary significantly only when the shelf width becomes smaller than R. On the deep water open boundary, the model uses static heights. This boundary condition is useful but not completely accurate; hence, we want the boundary as far removed from the coast as possible to reduce the effects of errors.

[36] In a homogeneous sea, pressure gradient effects reach the basin's bottom immediately; however, coastal surges resulting from the wind stress driving force are greater than surges from the pressure gradient driving forces, at least for tropical storms. Also, mass adjustments in a stratified sea, plus thermoclines, limit dynamic effects from driving forces to shallow surface layers not too great in depth, at least during the transient state of surge generation.

## Small Shelf Widths

There are some areas along the United States where the Continental Shelf is almost nonexistent, notably between the Florida Keys and West Palm Beach. The dynamic model, limited in its present state, would prefer to neglect these areas. However, from the viewpoint of the operational surge forecaster, this attitude is unacceptable. So, we here are forced to compromise as well as to improvise.

To form a usable shelf for the basin, we begin with the depth profiles off the Continential Shelf, as they exist for the first few miles from shore, until the 300-ft depth curve is reached. We then compromise our basin with a false, constant shelf depth of 300 ft for the remainder of the basin's length. Such severe depth changes at the coast, however, create special problems at one or both of the two false lateral boundaries that truncate our basin on the oceanside. The lateral boundary condition admits reflected[37] waves in the basin; with severe depth changes these reflected waves reach large amplitudes and move rapidly to the middle of the basin. To alleviate this situation, we improvise a platform or shallow depth profile normal to the coast at the lateral boundary and taper[38] the platform down to extreme depth values along the coast well before arriving at the basin's center. But false tapering depths along the shore and near a lateral boundary can form their own system of trapped waves which eventually corrupts the numerical solution. To prevent this effect, we limit the computation, stopping it well before the solution can be corrupted with these waves; empirical computations give a usable span of 10 to 12 hr in real time. This means that the computations here are less reliable for very slow storms.

We remark that the axis of Biscayne Bay, along the southeast coast of Florida, is larger than the diameter of most storms. It is a shallow area abutting a shelf of small width. The adjacent coastal areas are densely populated. Because of these factors, an attempt is made to incorporate the bay in the model; of course, we cannot do this precisely because of curvilinear coasts and the surrounding islands. It is unnecessary to apply a qualitative bay correction onto the computations here, but the model cannot account for local variations in the surge due to abrupt, local terrain changes.

The above techniques are provisional and have not been fully tested for all conceivable situations. So, we can expect unforseen problems to arise. The model tries to accommodate a variety of situations, but unusual conditions may precipitate an untenable state; the model then gives up in despair and produces instability. If or when this arises, the following guides will help for a new computation attempt.

---

[37] Clearly, we need here a radiation type boundary condition that is transparent for a <u>group</u> of traveling waves. This would be an interesting research project for the future.

[38] The tapering depths have a shoaling effect on waves traveling toward the shallow platform, and bottom stress dampens the shoaled waves. The trick here is to taper the shallow platform so that dampening effects are significant on all the shoaled waves; we do this by empirical tests with the model.

1. Let the storm track strike the coast at a less acute angle, consistent with meteorological accuracy.

2. Let the speed of the storm be as large as possible, consistent with meteorological accuracy.

3. Let the size of the storm be as large as possible, consistent with meteorological accuracy.

## E. Astronomical Tide

The tide tables, issued by the National Ocean Survey (NOS), give times and heights of high and low waters with respect to a datum. This datum, along the United States coasts of our interest, is MLW. We note that nautical charts published by the NOS for this area give depth soundings below MLW. This system is used by mariners for navigation purposes in which the lowest expected waters are of great interest.

The surge forecaster has a slightly different outlook; to him, highest expected waters are of great interest. His datum is MSL. The charts he uses give land contour elevations[39] above geodetic MSL; for this reason, we prepare astronomical tide predictions with respect to local MSL rather than MLW. The predicted tide plus computed surge (i.e., total storm tide) can then be directly compared with land contours to determine areas of inundation along the coast.

It would be better if we could always be this direct, but there are two anomolies here that sometimes can be significant.

1. Local MSL is not invariant with time.

2. The constituents Sa and SSa (annual and semiannual variations of the astronomical tide) are not always representative of actual conditions.

In almost all cases, local MSL changes slightly with the years; hence, land-contoured charts should be representative of the coast regardless of the year of issue. However, there are some special areas where changes in local MSL may be significant through the years. Thus, it may be wise for the surge forecaster to check the survey year of his chart and correct its sea-level datum to current or local MSL. Information on the relationship between geodetic and local tidal datum can be obtained from the NOS.

Sa and SSa presumably are measures of the seasonal changes of the sea-surface height at a tide station, caused by seasonal changes of the earth's meteorology. Figure 19 illustrates the amplitudes of these changes at a selected station for 1 yr; note that the peak amplitude occurs during the U.S. hurricane season. The curve is a best fit average with significant variance; it does not always represent the current state of affairs. For safety, it is suggested that normal predicted tide, in the coastal area of expected land-

[39] The NOS charts give some land elevations with respect to MHW (mean high water).

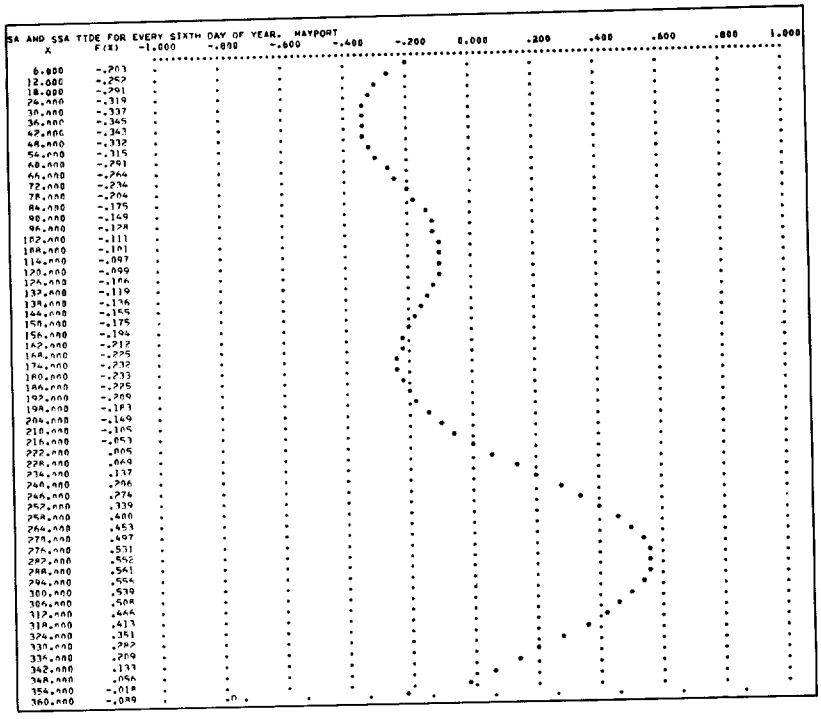


Figure 19.--Yearly variation of sea level at Mayport, Fla., derived from SSA (solar semiannual) and SA (solar annual) tide constituents. F(X) = SSA + SA.

fall, be compared with observed tide for several days before landfall (Harris 1958). If there is a trend in the comparison, then it can be incorporated with the predicted tide at the time of landfall.

A potentially dangerous situation occurs when both the peak meteorological and astronomical tides occur at or nearly at the same time. This situation generates larger total surges. From tide tables, we do know when peak semi-diurnal or diurnal astronomical tides occur; but peak meteorological tide is another story. Because of the state of the art in weather forecasting, we are not certain to the nearest hour when landfall will occur; also, we have given no criteria for the arrival time of peak meteorological tide with respect to landfall time. This arrival time depends in a complex manner on meteorological parameters, especially vector storm motion and the sea's bathymetry about the landfall point. In general we can say:

1. The peak meteorological surge occurs <u>before</u> landfall with slower moving storms (storms moving at speeds less than 20 mi/hr).

2. The peak meteorological surge occurs <u>after</u> landfall for faster moving storms (storms moving at speeds greater than 20 mi/hr).

3. In almost all cases, the time interval between peak surge and landfall is less than 1 hr.

For practical operational purposes, we can assume that peak surge and landfall occur simultaneously.

The probability of simultaneous occurrence of the two peaks is the same no matter what the storm speed, providing the storm is not stationary. We remark on a property of slow-moving storms; the duration of upper surges on the surge profile is long, sometimes even longer than a tidal period. Thus when dealing with very slow storms (speeds less than 10 mi/hr), the highest combined surge is virtually guaranteed to be larger than peak meteorological surge. But with fast-moving storms (speeds greater than 20 mi/hr), the duration of high surges is short, sometimes much shorter than a tidal period. Therefore, if astronomical tide is to be appended to meteorological tide with any reliability, we must have a reliable landfall time--say, to within $\pm 2$ hr for a semidiurnal tide and $\pm 3$ hr for a diurnal tide.

(Continued from inside front cover)

WBTM TDL 27 An Operational Method for Objectively Forecasting Probability of Precipitation. Harry R. Glahn and Dale A. Lowry, October 1969. (PB-188 660)

WBTM TDL 28 Techniques for Forecasting Low Water Occurrences at Baltimore and Norfolk. Lt. (jg) James M. McClelland, USESSA, March 1970. (PB-191 744)

WBTM TDL 29 A Method for Predicting Surface Winds. Harry R. Glahn, March 1970. (PB-191 745)

WBTM TDL 30 Summary of Selected Reference Material on the Oceanographic Phenomena of Tides, Storm Surges, Waves, and Breakers. Arthur N. Pore, May 1970. (PB-193 449)

WBTM TDL 31 Persistence of Precipitation at 108 Cities in the Conterminous United States. Donald L. Jorgensen and William H. Klein, May 1970. (PB-193 599)

WBTM TDL 32 Computer-Produced Worded Forecasts. Harry R. Glahn, June 1970. (PB-194 262)

WBTM TDL 33 Calculation of Precipitable Water. L. P. Harrison, June 1970. (PB-193 600)

WBTM TDL 34 An Objective Method for Forecasting Winds Over Lake Erie and Lake Ontario. Celso S. Barrientos, August 1970. (PB-194 586)

WBTM TDL 35 A Probabilistic Prediction in Meteorology: A Bibliography. A. H. Murphy and R. A. Allen, June 1970. (PB-194 415)

WBTM TDL 36 Current High Altitude Observations--Investigation and Possible Improvement. M. A. Alaka and R. C. Elvander, July 1970. (Com-71-00003)

NOAA Technical Memoranda

NWS TDL 37 Prediction of Surface Dew Point Temperatures. R. C. Elvander, January 1971. (Com-71-00253)

NWS TDL 38 Objectively Computed Surface Diagnostic Fields. Robert J. Bermowitz, February 1971. (Com-71-00301)

NWS TDL 39 Computer Prediction of Precipitation Probability for 108 Cities in the United States. William H. Klein, February 1971. (Com-71-00249)

NWS TDL 40 Wave Climatology for the Great Lakes. N. A. Pore, J. M. McClelland, and C. S. Barrientos, February 1971. (Com-71-00368)

NWS TDL 41 Twice-Daily Mean Monthly Heights in the Troposphere Over North America and Vicinity. August F. Korte, June 1971. (Com-71-00826)

NWS TDL 42 Some Experiments With A Fine-Mesh 500-Millibar Barotropic Model. Robert J. Bermowitz, August 1971. (COM-71-00958)

NWS TDL 43 Air-Sea Energy Exchange in Lagrangian Temperature and Dew Point Forecasts. Ronald M. Reap, October 1971. (COM-71-01112)

NWS TDL 44 Use of Surface Observations in Boundary-Layer Analysis. H. Michael Mogil and William D. Bonner, March 1972.

NWS TDL 45 The Use of Model Output Statistics (MOS) To Estimate Daily Maximum Temperatures. Lt. (jg) John R. Annett, NOAA, Harry R. Glahn, and Dale A. Lowry, March 1972.

COASTAL ZONE
INFORMATION CENTER

NOAA COASTAL SERVICES CENTER LIBRARY
3 6668 00002 9175